Edition III

Sheet Steel Handbook

Design and fabrication in high strength sheet steel

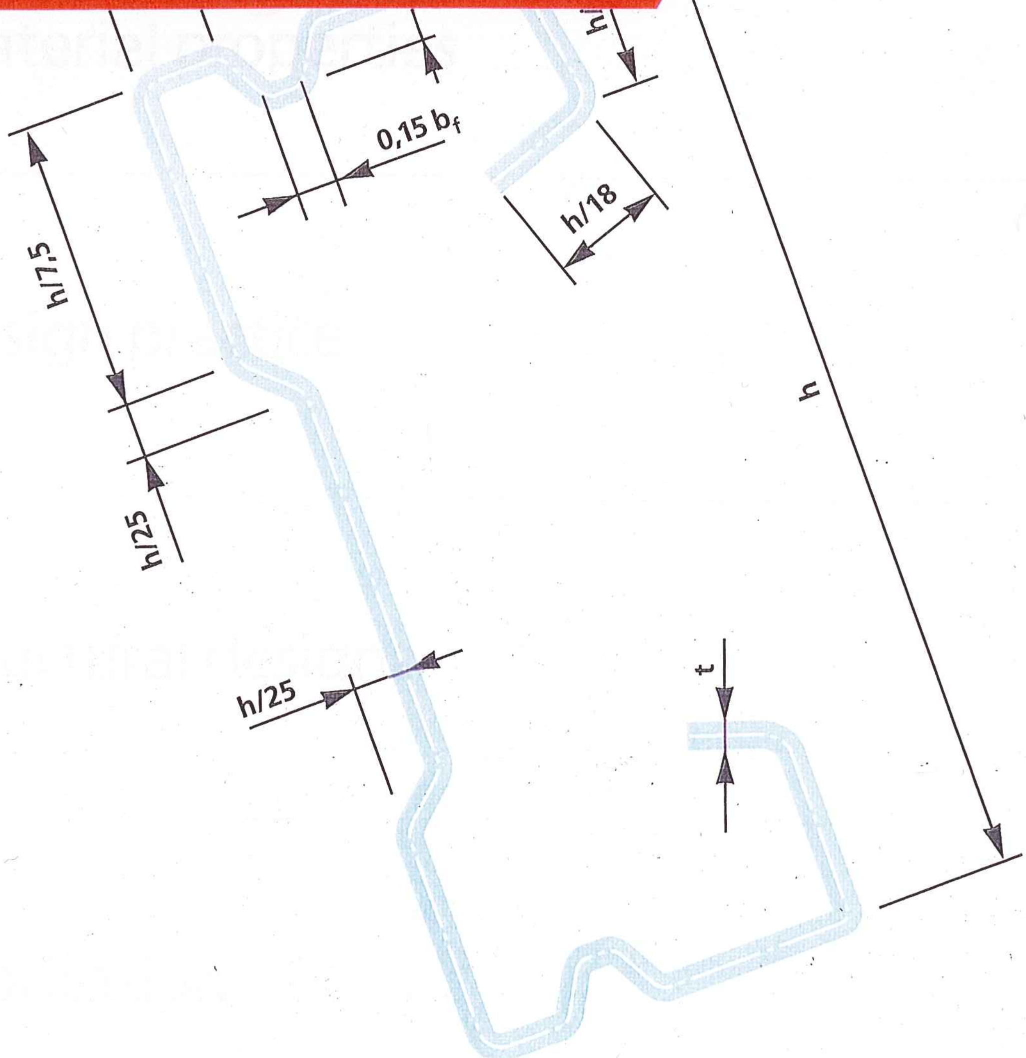

SSAB TUNNPLÅT

4.6 Design with respect to fatigue

Increased material utilization has necessitated increased consideration of the problem of fatigue. Subsection 4.6.1 gives a general introduction to this problem, but this is not essential reading for the subsection on design, 4.6.2, to be made use of. The latter is mainly based on the new Swedish Regulations for Steel Structures BSK, which is, in turn, substantially the same as the previous Swedish Regulations for Welded Steel Structures StBK-N2 (Ref. 4:25).

Summary and general recommendations

Factors which affect fatigue

- Fatigue is a process in which a material breaks down and cracks are formed on repeated loading. Stresses are often much lower than the yield strength of the material. In practice, there is a risk of fatigue when the number of load cycles exceeds 10^3.

- In the *first place,* fatigue strength is a function of the stress concentration effects, the number of load cycles and the shape of the load spectrum.

- In the *second place,* the fatigue strength is influenced by the static strength, mean stress, residual welding stresses, corrosion of the parent material, sheet thickness, temperature and loading frequency.

- Since the load spectrum and the number of loading cycles have a great effect on fatigue strength, it is well worth carrying out an accurate load analysis prior to design.

- Structures should be checked in particular with respect to resonance and vibration phenomena. These can give rise to many stress cycles of large amplitude and can considerably shorten the fatigue life.

Design aspects, stress concentration effects

- The fatigue characteristics of welded joints are to a large extent governed by the macro and micro geometry of the weld, i.e. by the weld quality.

- The designer, production engineer and the individual welder have a decisive influence on the fatigue characteristics of a welded structure.

- Design so that the flow of stress is as uniform as possible. Avoid abrupt changes in section and large changes in stiffness.

- As far as possible, use butt welds instead of fillet welds in highly stressed regions. If fillet welds are used, these shall be designed so that initiation of fatigue cracking at the root is avoided.

- Do not place welds, even non-loadcarrying ones, in parts of the cross section where fatigue stresses are high. If possible, apply loads to beams at the neutral axis.

- Minimize local stress concentrations near welds, i.e. endeavour to cut down the quantity of excess weld metal, to make fillet welds concave with smooth transitions between weld and parent metal, and to minimize undercut.

- Choose the best welding position, downhand if possible. Avoid axial or angular misalignment because this can give rise to large additional stresses. Good weld quality results in good overall economy.

- The significance of internal defects in welds must be seen in relation to the stress concentration effect of surface defects. Surface defects are normally more dangerous than internal ones (by a factor of 4–5).

- Do not forget to impress on the individual welder the importance of good weld quality!

The influence of material

- The fatigue strength of non-welded material is proportional to the static strength of the steel.

- Cracks are rapidly initiated near welds, and in such a case the life is mainly determined by crack growth. The fatigue strength of a welded joint acted upon by a load of constant amplitude and a large number of load cycles ($N > 10^5$) is therefore independent of the static strength of the parent material.

- High strength steels can however be used to good effect in welded structures subject to fatigue loading, where mean stresses are high, the number of load cycles moderate and the applied load spectrum contains relatively few high load cycles.

Residual welding stresses

- Residual welding stresses can be as high as the yield strength, and are normally tensile in critical regions. Because of this it is the stress range σ_r which is the significant parameter with regard to the fatigue of welded joints.

- Stress relief heat treatment can increase fatigue strength (by approx 25% for $R = -1$) if some part of the nominal stress cycle is compressive stress.

Environmental effects

- A corrosive environment lowers fatigue strength by up to 40%. Even in unwelded structures increased tensile properties no longer exert any positive influence. Cathodic protection and surface treatment improve fatigue strength.

— Batch hot dip zinc coating can reduce fatigue strength. The higher the strength of the parent material, the greater this reduction. On the whole, however, a material with corrosion protection has a higher fatigue strength in a corrosive environment than one which has received no treatment.

Methods of increasing fatigue strength

— The fatigue strength of welded joints can be increased in various ways:

1. Reduction of stress concentration effects by changing structural details and by ensuring that quality of fabrication is high.
2. Grinding or TIG dressing of highly stressed welds.
3. Stress relief heat treatment (if $R < 0$).

4.6.1 Factors which influence fatigue strength

In fatigue the material gradually breaks down owing to repeated loading. Fatigue is characterized by cracking in regions of high local stresses (stress concentration effect), regions which are in most cases "safe" under static loading.

Fatigue is characterized by little plastic deformation, and fatigue cracks are therefore difficult to detect. The fracture surface is of oystershell appearance, usually with clearly discernible arrest lines showing the progress of the fatigue crack.

The fatigue process is usually divided into initiation and growth of the crack. From the standpoint of metal physics, these phases are different processes. Generally speaking, the initiation phase dominates where there is little stress concentration, and the crack growth phase where stress concentration effects are considerable, for instance near welds.

The fatigue strength is equal to the maximum stress variation a material can withstand without failing in fatigue after a certain number of stress cycles. The relationship between fatigue strength and life (number of load cycles to failure) is given by the Wöhler curve. Note that the Wöhler curve usually represents a mean value of the fatigue strength (50% probability of failure) and that the scatter about the curve may be considerable. See Fig. 4.6.1.

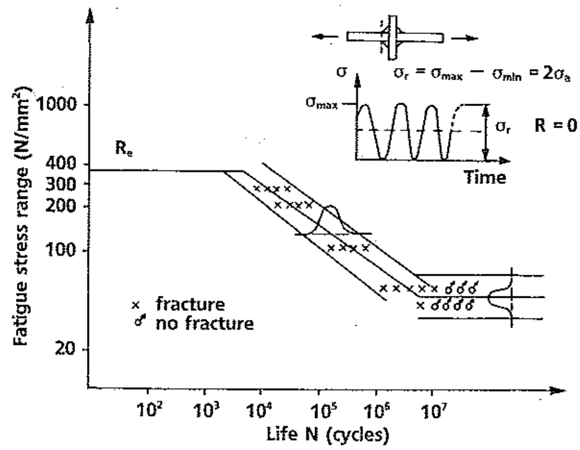

Fig. 4.6.1 *Typical Wöhler curve (S-N curve) with scatter band*

The fatigue strength is affected by a large number of factors, many of which are difficult to derive physically and to quantify. Knowledge relating to fatigue has therefore been acquired by means of extensive testing programmes.

Stress concentration effects, the number of load cycles and the shape of the load spectrum are the three factors which primarily influence fatigue strength. Other factors are the static strength of the parent material, mean stress (residual stresses), sheet thickness, environment, metallic coatings, temperature and loading frequency.

The effect of the factors which influence fatigue strength increases as the number of load cycles increases. For this reason, a structure is not usually regarded as subject to fatigue loading until the number of load cycles exceeds 10^3 during its life.

Definitions

The most common terms used to describe the fatigue stress are defined in Fig. 4.6.2.

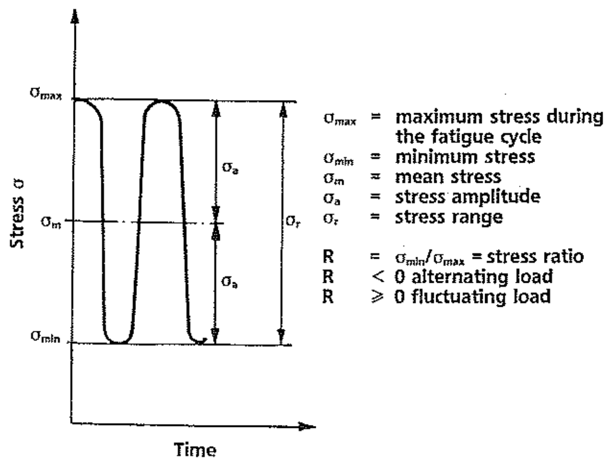

Fig. 4.6.2 *Definitions of terms relating to stresses in a fatigue cycle*

The effect of load

Number of load cycles

Fatigue strength decreases as the endurance increases. This reduction is small in parent material without stress concentrations but it is considerable where the stress concentration factor has a high value, Fig. 4.6.3. In a fillet welded joint, for instance, the fatigue strength at $2 \cdot 10^6$ cycles may be only 20% of that at 10^4 cycles.

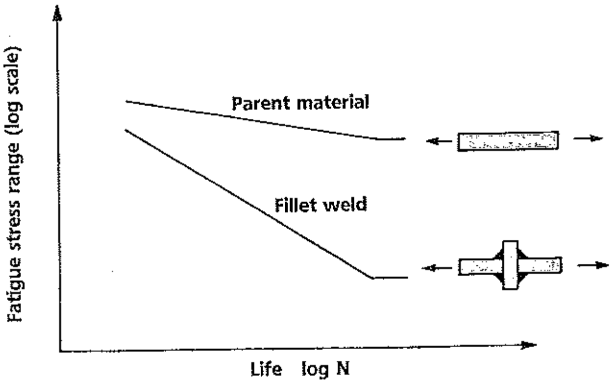

Fig. 4.6.3 *Typical Wöhler curves for parent material without stress concentrations and for a fillet welded joint*

It is very expensive to ensure that the fatigue stress is at all points less than the fatigue limit. Many structures are exposed to a moderate number of load cycles, and it is then important to design for a limited life (the sloping portion of the Wöhler curve) in order to obtain an optimum structure.

Load spectrum

Most structures are subjected to loads which vary with time in an irregular, often random, fashion, i.e. to a load spectrum. Examples of this are an excavator working in varying terrain conditions, or a crane which hoists different loads at different times, Fig. 4.6.4.

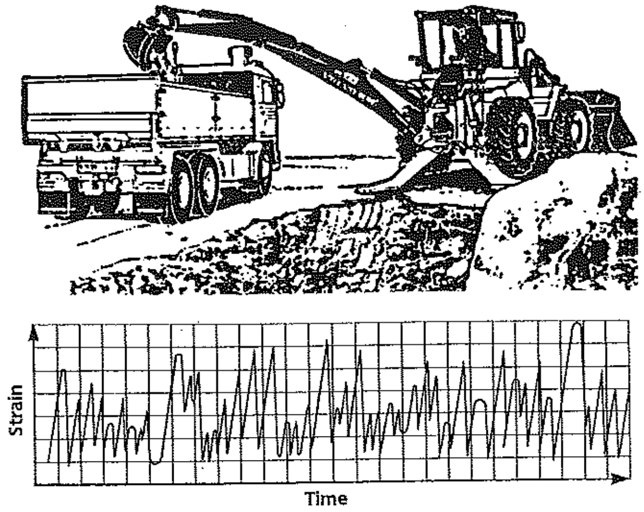

Fig. 4.6.4 *Transducer signals from an excavator*

To design for maximum load in each cycle (full load spectrum, $\varkappa = 1$) would result in gross overdesign. For a usual load spectrum, $\varkappa = 1/2$, the fatigue strength is about 70% higher than that for a full spectrum, $\varkappa = 1$; see Fig. 4.6.5. Together with what has been said above regarding limited life, this emphasizes the importance of a correct load analysis.

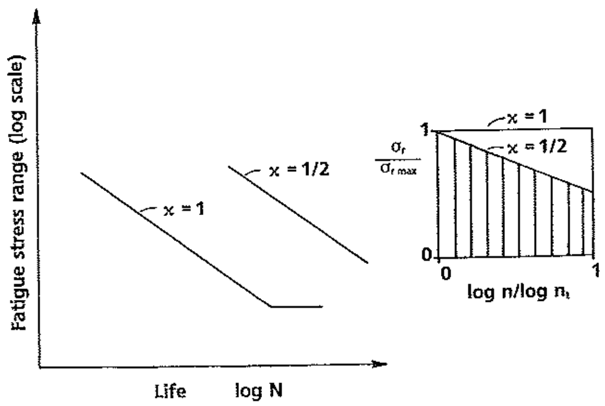

Fig. 4.6.5 *The effect of load spectrum*

The load spectrum in question is determined by measuring or estimating the actual loads. The load spectrum is then compared with standardized values or an analysis carried out in accordance with the Palmgren-Miner rule. An analysis of the measured load spectrum can be made in many different ways, such as level crossing, peak counting or rainflow or range pair analysis. For welded joints where the stress range is usually the significant parameter, range pair analysis is mostly used. A certain measure of discretion must be applied in using this method when signals are similar to pure sine wave signals (Ref. 4:26, 4:27).

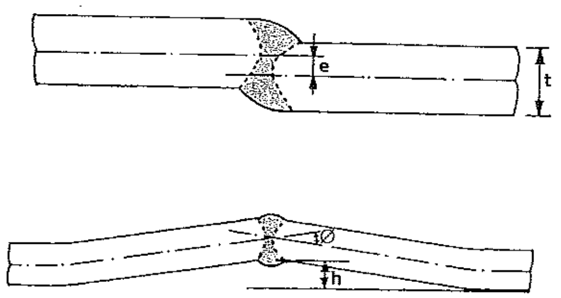

Fig. 4.6.9 *Axial and angular misalignment*

Microgeometrical stress concentration effects also arise as a result of defects such as cracks, incomplete root penetration (lack of side fusion, lack of root fusion), porosity and slag inclusions, Fig. 4.6.10.

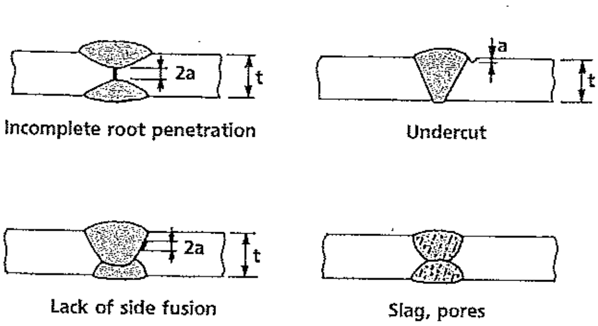

Fig. 4.6.10 *Examples of welding defects*

It is essential to know what level of defects can be tolerated in a joint class C. For undercut, lack of side fusion, slag inclusions and porosity there are certain typical values (Ref. 4:29):

Type of joint	Undercut, surface defect depth (a/t)	Internal defect height (2a/t)	Slag inclusion length (mm)	Porosity volume (%)
Butt weld	0.02	0.1–0.2	2	2
Fillet weld	0.07	0.2–0.3	15	5

Cracks and similar defects (lack of side and root fusion) larger than the above should be subjected to fracture mechanics analysis. See section 4.7.

Remember that stress concentration is the factor which can be most easily influenced by the designer and the production engineer. Try and make the stress flow uniform, select a welded joint with the highest possible joint class, and select welding techniques, electrodes and welding positions which produce smooth weld toes.

The effect of material tensile strength

Parent material with and without mechanical stress concentrations

The fatigue strength of material without stress concentrations and with moderate mechanical stress concentrations increases with increasing static strength (R_e, R_m). The following approximate rules of thumb are applied for as-rolled steel sheet without stress concentrations at $N = 2 \cdot 10^6$ cycles.

Fluctuating tensile load, $R = 0$:

$f_r \approx 0.7\ R_m$ for $R_e/R_m \geqslant 0.7$

$f_r \approx R_e$ for $R_e/R_m < 0.7$

Alternating load, $R = -1$:

$f_r \approx 0.8\ R_m$

Owing to greater notch sensitivity, the significance of surface quality increases with increasing static strength. Steels of the highest strengths ($R_e \geqslant 500$ N/mm²) in the as-rolled condition may therefore have a slightly lower fatigue strength than that given by the above rules of thumb. Fig. 4.6.11 gives values of the fatigue strength for DOMEX and DOCOL steels in the as-rolled condition.

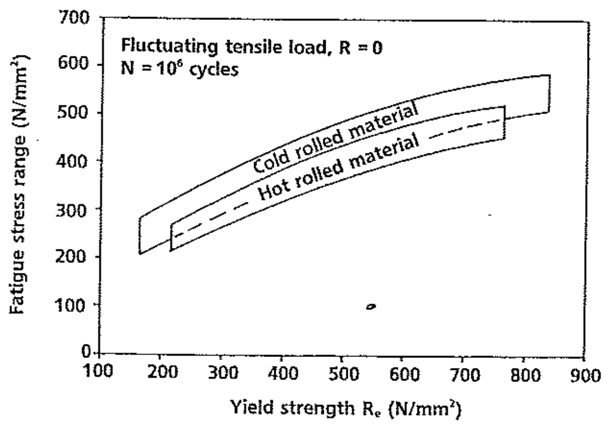

Fig. 4.6.11 *Fatigue strength of parent material in as-rolled condition*

In the case of sheet the yield strength can be raised by strain hardening and/or bake hardening (e.g. in pressing and curing the paint in the automotive industry). Increased yield strength usually results in increased fatigue strength by an amount corresponding to the effect of the yield strength increase (Ref 4:30). In mechanically notched structures subject to high load variations the plastic strains may be so large that cyclic softening occurs. The positive effect of strain and bake hardening is then reduced and may in some cases disappear (Ref. 4:31).

Evaluation of the load spectrum on the basis of measurements is nowadays usually carried out automatically using special measurement and analysis equipment.

Load type, mean stress

Owing to the stress gradient, the fatigue strength of unnotched test bars is usually approx 20% higher in bending than in tension.

The influence of the mean stress, which is usually described in a Goodman, Haigh or $\sigma_r - \sigma_m$ diagram, is in practice greatest for $R < 0$ (Fig. 4.6.6). For welded joints in which there are residual welding stresses, the stress range σ_r is the significant parameter. Locally at the weld, the stress range varies from the yield strength downwards regardless of the nominal value of R.

The following rule of thumb may be used for conversion of the fatigue strength between loading combinations with different values of R if the residual stresses are small.

$$\frac{f_r\,(R = -1)}{f_r\,(R = 0)} \approx 1.25$$

$$\frac{f_r\,(R = 0.5)}{f_r\,(R = 0)} \approx 0.85$$

For welded joints in high strength steel the fatigue strength is largely independent of the mean stress if $R > 0$, i.e. the value of the second ratio above is approximately equal to 1.

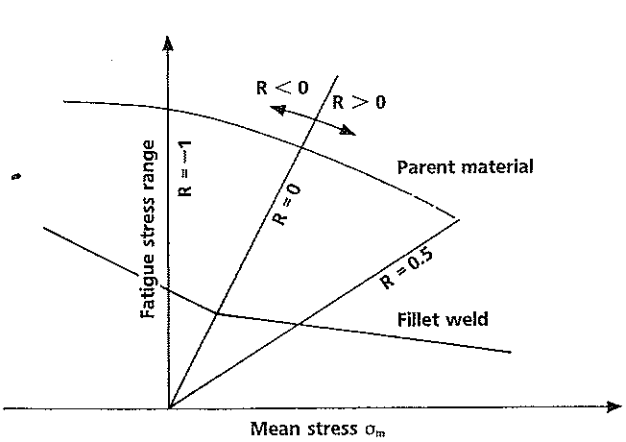

Fig. 4.6.6 *The effect of mean stress on fatigue strength*

Stress concentration effect

Stress concentrations reduce the fatigue strength. The more the flow of stress is disrupted, the greater is the stress concentration effect. For *mechanical stress concentrations* such as holes the stress concentration effect is usually assessed with reference to the stress concentration factor K_t and the notch sensitivity q, and a fatigue strength reduction factor K_f calculated from these. In *welded structures* the stress concentration conditions are more complicated and made up of macro and microgeometrical stress concentration effects. It is usual for a joint class C to be defined. The value of C is the characteristic fatigue strength in N/mm^2 of the joint at $2 \cdot 10^6$ cycles. Typical values of C are C = 80 for holes, C = 90 for butt welds and C = 45 − 56 for fillet welds. The macrogeometrical stress concentration effect in a welded joint is exemplified for different types of joints in Fig. 4.6.7, and the microgeometrical effect by the undercut in Fig. 4.6.8.

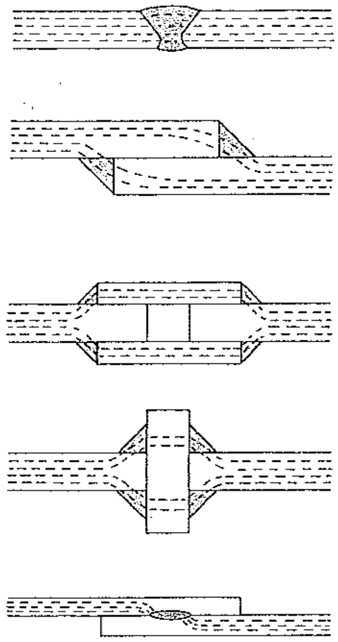

Fig. 4.6.7 *Macrogeometrical stress concentration effect*

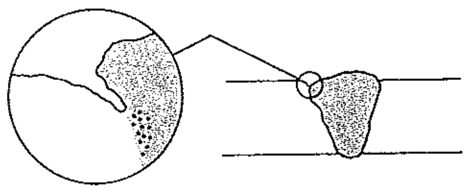

Fig. 4.6.8 *Microgeometrical stress concentration effect in a butt welded joint. The enlarged detail shows an undercut with underlying slag inclusions*

Angular and axial misalignment introduce bending stresses and reduce fatigue strength, Fig. 4.6.9. For axial misalignment, $K_t = 1 + 3e/t$. It is normally considered that $K_t < 1.3$ is included in the joint class C, i.e. $e < t/10$ is permissible. For angular misalignment the calculations are more complicated. Note that a small angular error of a few degrees may double the local stress (Ref. 4:28).

Welded joints

Undercuts and other defects in welded joints are usually so sharp that they may be regarded as "cracks", and life is therefore mainly governed by crack growth. Since the resistance of high strength steels to crack growth is the same as that of mild steels, the welded joints also have the same fatigue strength when acted upon by constant amplitude loads and high numbers of load cycles. This has nothing to do with the greater notch sensitivity of the high strength steels.

The above *does not imply* that high strength steels are of no interest in welded structures subject to fatigue loading. Welds can be positioned in regions of lower stress, for instance loads can be applied to the webs of beams by plug welds. High strength steels can also be utilized in structures designed for low endurances, at high mean stresses and in conjunction with spectrum loading where the applied load spectra contain relatively few high load cycles. The reason in the last case is both that the limit in number of cycles between static and fatigue design is moved towards higher endurances, and that high load peaks give rise to higher retardation effects in high strength steels than in mild steels.

High strength steels are also advantageous in cases where the fatigue strength of the welded joint can be improved, for instance by grinding, peening or TIG dressing. In spot welded joints fatigue strength can be raised by reducing the spot pitch or increasing the weld nugget diameter (Ref. 4:32).

Residual welding stresses – stress relief heat treatment

There is a large difference in fatigue strength between regions with tensile and compressive residual stresses. The positive effect of introducing compressive residual stresses when axles are case hardened, or in conjunction with peening, is well documented.

In practice it is assumed that the residual welding stresses are tensile stresses of the same order as the yield strength, Fig. 4.6.12.

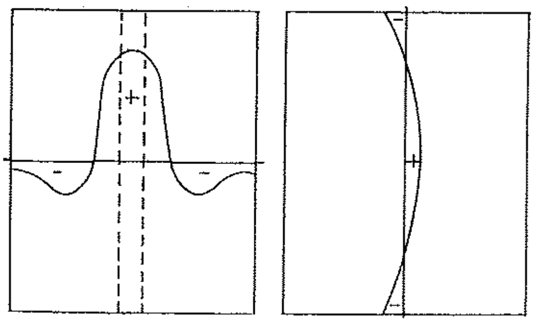

Fig. 4.6.12 *Usual distribution of residual stresses across and along a butt weld*

Since the fatigue strength for $R > 0$ does not increase appreciably as R decreases, Fig. 4.6.6, the effect of stress relief heat treatment at fluctuating tensile loading ($R \geqslant 0$) is marginal. If, on the other hand, a certain proportion of the nominal stress cycle is compressive ($R < 0$), stress relief heat treatment usually produces a positive effect; fatigue strength is increased by approx 25% under a pure alternating load, $R = -1$.

Sheet thickness

As the sheet thickness decreases, fatigue strength increases. For non-welded structures this is ascribed to the statistical volume effect. The smaller the stressed volume, the lower the probability of failure and the higher the fatigue strength, Fig. 4.6.13. This also explains why the fatigue strength in bending is greater than in tension (approx 20%).

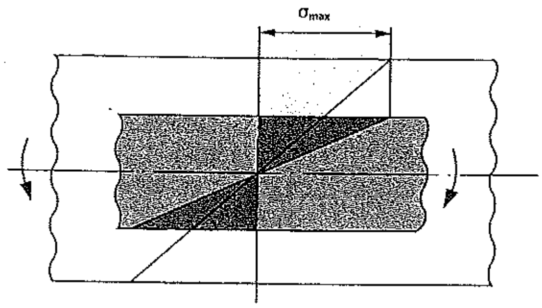

Fig. 4.6.13 *The effect of thickness on the stress gradient in bending*

In welded joints there is another type of thickness effect which can be derived by fracture mechanics (Ref. 4:33). The smaller the material thickness, the smaller the region subject to high stress concentration effects near the weld, i.e. crack growth occurs over a shorter distance at high stress. The thickness effect in fillet welds is usually described by the expression

$$f_r = f_{ro}\left(\frac{t_o}{t}\right)^{\alpha}$$

where the value of α is between 0.10 and 0.25.

Existing design rules, for instance in BSK, are based on experimental results from test specimens with sheet thicknesses around 15 mm. It is therefore reasonable to make t_o = 15 mm if there is no other documentation available. The fatigue strength of 5 mm sheet is then approx 20% higher than that of 15 mm sheet.

Temperature

Over the temperature range −100 to + 400°C, the effect of temperature on fatigue strength is only marginal. Above 400°C creep phenomena appear (normal structural grade steels), and creep and fatigue must be treated together.

Temperature variations in structures subject to temperature gradients may result in reversible plastic strains, and the number of strain cycles to failure is small. Strain cycling fatigue theories, for instance that proposed by Manson-Coffin, can then be used to determine life (Ref. 4:34). The ductility of the material is of great significance at large strains.

Note the risk due to temperature changes when materials with different coefficients of linear expansion are used in the same structure (e.g. carbon steel and stainless steel)!

Corrosion fatigue, corrosion protection

The term corrosion fatigue usually refers to the cases where a corrosive environment appreciably reduces the time to crack initiation or accelerates crack growth under fatigue loading. Corrosion fatigue gives rise to a lower fatigue strength than the in-air fatigue strength of an already corroded material, Fig. 4.6.14.

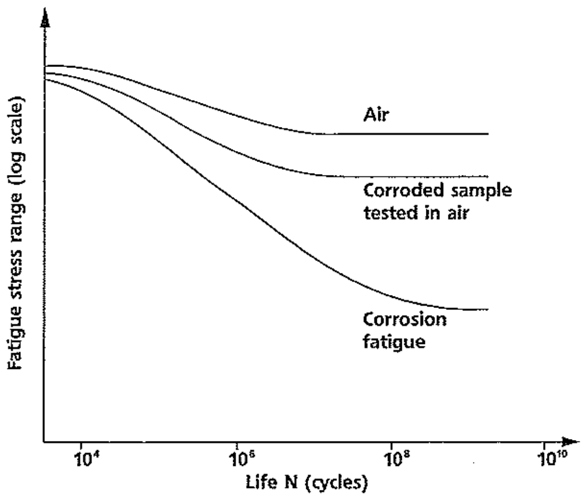

Fig. 4.6.14 *Corrosion fatigue compared with fatigue of an already corroded and a non-corroded material*

Painted structures in a normal environment are not usually deemed to be in danger of corrosion fatigue. The phenomenon is usually considered only in really severe environments, for instance offshore.

The factors to which the greatest attention must be paid in a corrosive environment, compared with conditions in air, are that load frequency (time) is of greater significance, that the material, even when not welded, can cease to exert an influence, and that the fatigue limit is lowered.

A reduction of fatigue strength by up to 40% in salt water compared with air has been reported, Fig. 4.6.15.

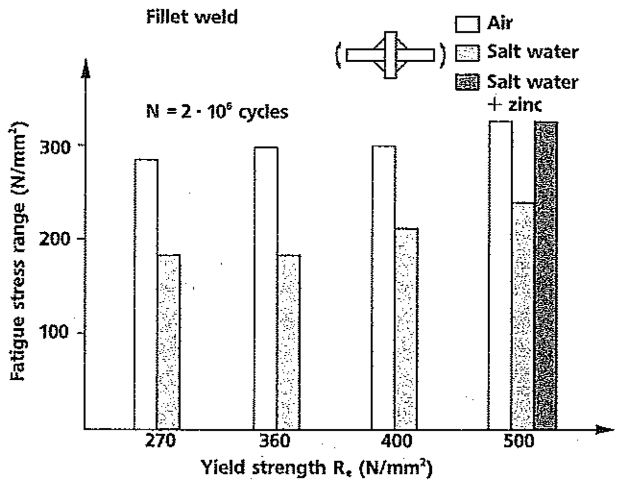

Fig. 4.6.15 *Results of fatigue tests on fillet welded joints in salt water*

Cathodic protection, for instance sacrificial anodes of zinc, can give a fatigue strength similar to the values in air. See Fig. 4.6.15.

Metallic coating usually provides good protection against corrosion fatigue but may itself reduce fatigue strength to a certain extent.

The way batch hot dip zinc coating affects the fatigue strength of parent material without stress concentrations is shown in Fig. 4.6.16.

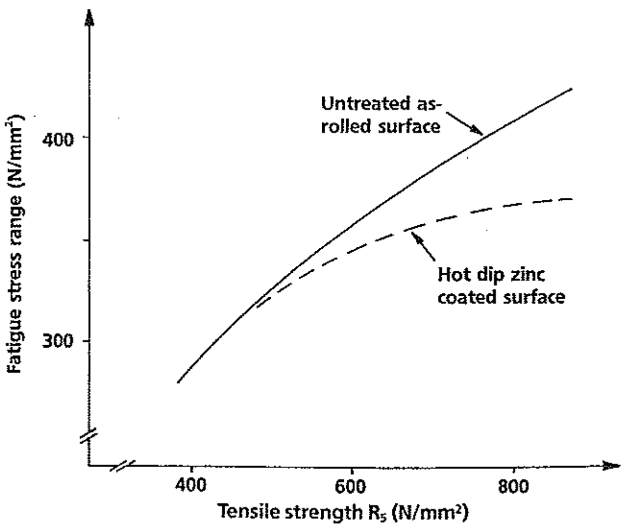

Fig. 4.6.16 *The effect of batch hot dip zinc coating on fatigue strength (Ref. 4:35)*

4.6.2 Design with respect to fatigue failure

The Swedish Regulations for Welded Steel Structures StBK-N2 contain one of the first modern rules for design with respect to fatigue and have therefore been used for a long time outside their formal field of application. Swedish Regulations for Steel Structures BSK which have now superseded StBK-N2 are based on the same principles, but they also formally permit a differentiated safety approach of the kind which has for a long time been applied in the engineering industry.

This handbook is based on the principles of BSK (EC 3) with certain additions as regards joint classes for parent material and welded joints with a high degree of stress concentration. A thickness factor and data which will enable the failure risk level to be varied have also been introduced.

Conditions

The fatigue design procedure presented below assumes that the details have already been designed in broad outline, i.e. that the dimensions and steel grades are chosen and that welded joints have been positioned and designed in the most appropriate manner. The required life n_t (number of load cycles) is greater than 10^3 cycles (if $n_t < 10^3$ cycles the structure need not be checked for fatigue).

Calculation procedure

1. Choice of *point* for analysis
   Identify critical joints and select the weld *Quality Level* (Swedish Standard SS 06 61 01*). Determine the stress concentration effect, i.e. *joint class C*, Fig. 4.6.27.

2. *Load analysis*
   Measure, calculate or estimate the load spectrum and calculate $\sigma_{r\,max}$. Determine *the spectrum parameter* $\varkappa$ in accordance with Fig. 4.6.18 – 20.

3. Determine the *characteristic fatigue strength f_{rk}* for the actual joint class C, spectrum parameter $\varkappa$ and number of cycles n_t Fig. 4.6.24.

3.1 Determine the *thickness factor φ_t* in accordance with Fig. 4.6.22.

3.2 Determine the *material factor φ_m* for non-heat affected parent material in accordance with Fig. 4.6.23. For heat affected material and oxygen cut edges, $\varphi_m = 1$.

3.3 Determine the *stress alternation factor φ_e* in accordance with Formula 4.6.8. If the residual stresses are not known or if $R > 0$, $\varphi_e = 1$.

4. Determine the *partial safety factor for design capacity γ_{mn}* in view of the consequences of failure, Fig. 4.6.25.

5. *Design criterion*

$$\sigma_r \gamma_f = \sigma_{rd} \leqslant f_{rd} = \frac{f_{rk}\,\varphi_t\,\varphi_m\,\varphi_e}{\gamma_{mn}} \qquad (4.6.1)$$

If $\sigma_{rd} > f_{rd}$, reduce the stress concentration or increase the dimensions. Repeat the calculation.

If it is the life which is to be calculated, put $f_{rd} = \sigma_{rd}$, and calculate f_{rk} in accordance with 5. above. After this determine n_t from Fig. 4.6.24.

A flow chart for the calculation procedure is given in Fig. 4.6.26.

* ISO/DIS 5817.3

NOTE!

Do not forget that maximum load must not exceed the static design capacity.

Comments and recommendations regarding the calculation procedure

1 Choice of calculation points, joint classes

It is important to find the critical points with respect to the nominal stress level (direction of principal stress) and stress concentration effect (C). Transverse fillet welds and the ends of welds, especially in combination with discontinuities in stiffness, are often critical regions.

The joint class C is equal to the characteristic fatigue strength (mean value less 2 standard deviations) for $n_t = 2 \cdot 10^6$ cycles and full load spectrum ($\varkappa = 1$).

C is determined using Fig. 4.6.27. The joint class set out takes account of macro and microgeometrical stress concentration effects, and there shall be no increase in nominal stress except in two special cases. The first refers to large eccentricities (> 10%) or angular misalignment in the welded joint when the bending stress component must be taken into consideration, and the second to interacting stress concentrations.

Where there are two interacting stress concentrations, the lowest value of C, reduced by one step, applies. Where there are more than two interacting stress concentrations, *the lowest value of C is reduced* two steps in the series of C values.

If C is lower than 35, either a higher weld Quality Level must be chosen or the joint must be redesigned.

A hole in the vicinity of a weld is considered to affect the joint class if the distance between the edge of the hole and the weld is less than the hole diameter. The effect of the hole is taken into account by *increasing the nominal stress* by the factor $\sqrt{200/C}$ where C is joint class for the hole according to Fig. 4.6.27. For a hole occupied by a normally tightened bolt, the value of C is to be increased by two steps.

In spot welded joints which transmit a shear force, the spot welds are, in addition to the shear force, also acted upon by a bending moment which increases the local stress.

In this case (joint configuration No 57 in Fig. 4.6.27) the joint class C is evaluated on the assumption that the characteristic design capacity per spot weld is calculated from Formula (4.6.2) (Ref. 4:36)

$$F_{rk} = \frac{3\, f_{rk}\, t}{\left(\frac{2}{\pi d} + \frac{3}{e}\right)} \qquad (4.6.2)$$

where t = sheet thickness
d = weld nugget diameter
e = weld pitch

Where there are several rows of spot welds, the design capacity per weld is reduced, see Fig. 4.4.2.

For spot welded beams (Cases 58 – 60 in Fig. 4.6.27a) the nominal stress is calculated by conventional beam theory. Current research indicates that the fatigue strength of non-loadcarrying spot welded joints (Cases 58 – 59) increases in proportion to the increase in strength of the sheet material.

For *mechanical stress raisers* which are not covered by Fig. 4.6.27, handbooks, e.g. that by Peterson (Ref. 4:37), can be used for the determination of the stress concentration factor K_t. C can then be determined approximately from Fig. 4.6.17 where r is the radius of the mechanical stress raiser.

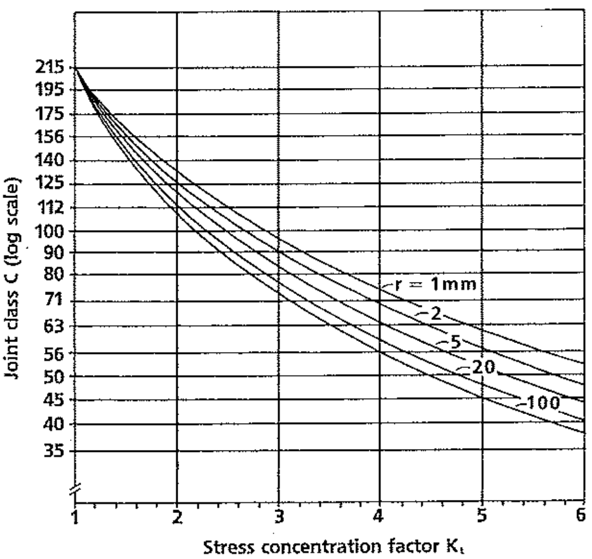

***Fig. 4.6.17** Joint class C as a function of the stress concentration factor K_t. r = radius of stress raiser*

Fig. 4.6.17 is based on the following expressions:

$$C = 215/K_f \qquad (4.6.3)$$

$$K_f = 1 + \frac{K_t - 1}{1 + \frac{0.6^*}{\sqrt{r}}} \qquad (4.6.4)$$

where r = radius (mm) of stress raiser

* Neuber parameter $\sqrt{A} = 0.6$
(for mild steel, $R_e = 220$ N/mm^2)

Note that in this case the effect of the material is allowed for separately by the material factor φ_m and not by different values of the Neuber parameter $\sqrt{A}$.

2 Load analysis

Correct load analysis is the most important, and usually the most difficult, part of design with respect to fatigue. A design based on the assumption that all load cycles are equal to the maximum often results in gross overdesign.

The load spectrum for a component can be measured over a number of representative working cycles. The measured load spectrum must then be converted into a characteristic load spectrum for the entire life. For some structures there are empirical values or values specified by the regulatory authorities, Fig. 4.6.18.

The 100 stress cycles with the highest values of σ_r and all stress cycles with design values of the stress range ($\sigma_r\gamma_f$) smaller than those corresponding to the fatigue limit ($n_t = 10^8$, $\varkappa = 1$) can be ignored in determining the design load spectrum.

The design load spectrum is then compared with the standardized load spectra set out in Fig. 4.6.19, and the spectrum parameter determined. See the example in Fig. 4.6.20.

Structure	$\varkappa$	n_t
Bridges	1/3	$2 \cdot 10^6$
Steel buildings	1/2	*
Mobile crane, hook operation	0-1/2	$2 \cdot 10^5$
Overhead crane in steelworks	2/3-1	*
Container crane	2/3	*
Ship bottom	0	10^8
Excavators (jib, dipper arm)	1/2-2/3	*
Vehicle frames:		
Dumpers, tippers	2/3	$2 \cdot 10^6$
Forestry machinery	1/2-2/3	*
Mobile crane chassis	0-1/2	*
Forks of fork lift trucks, sawmill handling plant	1/3	$2 \cdot 10^6$
Jibs of wheeled loaders:		
heavy duty, regular cycle	1/6-1/3	*
normal, variable duty	0-1/6	*

* Varies depending on application

***Fig. 4.6.18** Usual values of spectrum parameter $\varkappa$ and design load cycle number n_t*

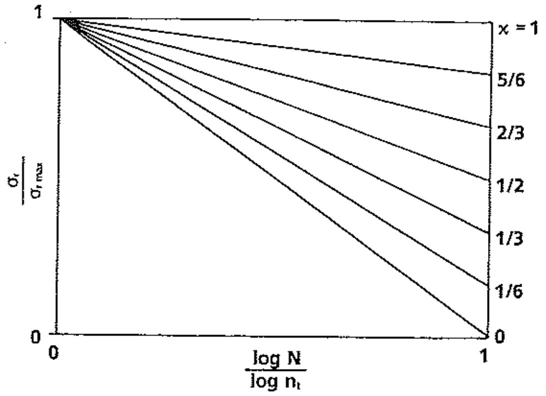

Fig. 4.6.19 *Standardized load spectra*

3 Characteristic fatigue strength f_{rk}

For a constant stress range ($\varkappa$ = 1) the characteristic fatigue strength is given by

$$f_{rk} = C\left(\frac{2 \cdot 10^6}{n_t}\right)^{1/m} \qquad n_t \leqslant 5 \cdot 10^6 \text{ cycles} \qquad (4.6.5)$$

$$f_{rk} = 0.4^{\left(\frac{1}{m}-\frac{1}{5}\right)}\, C\left(\frac{2 \cdot 10^6}{n_t}\right)^{1/5} \qquad 5 \cdot 10^6 < n_t < 10^8 \text{ cycles} \qquad (4.6.6)$$

For structures which are not appreciably affected by corrosion, the fatigue limit under constant amplitude loading is the same as the fatigue strength at $5 \cdot 10^6$ cycles ($f_{rk} = 0.4^{1/m}$ C). For other cases the corresponding value at 10^8 cycles ($f_{rk} = 0.25^{1/m}$ C) is chosen.

In order that realistic relationships should be obtained between f_{rk} and n_t for high joint classes, the slope of the Wöhler curve has been gradually reduced for C ⩾ 125, and at the same time more joint classes have been introduced (Ref. 4:35, 38 — 39). The selection of the slope m is such that the curves converge at $n_t = 10^3$ cycles and C = 112 (f_{rk} = 1410 N/mm²).

The slopes m for the different joint classes are then

C	35—112	125	140	156	175	195
m	3.0	3.14	3.29	3.45	3.64	3.84

The relationship between the characteristic value of the fatigue strength at constant stress range and the number of stress cycles is set out in Fig. 4.6.21.

a)

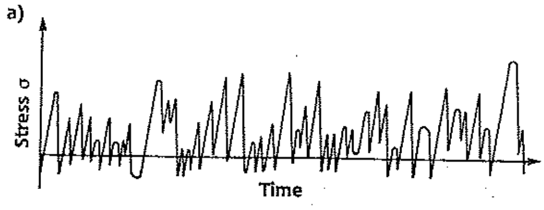

b)

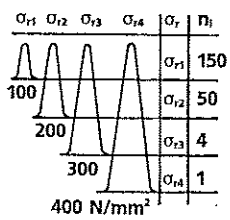

c)

i	σ_{ri} (N/mm²)	$\frac{\sigma_r}{\sigma_{r\,max}}$	$n_i\frac{n_t}{n_1}-100$	$\frac{\log N}{\log n_t}$
1	100	0.25	99,900	1.000
2	200	0.50	33,233	0.904
3	300	0.75	2,567	0.682
4	400	1.00	567	0.551

d)

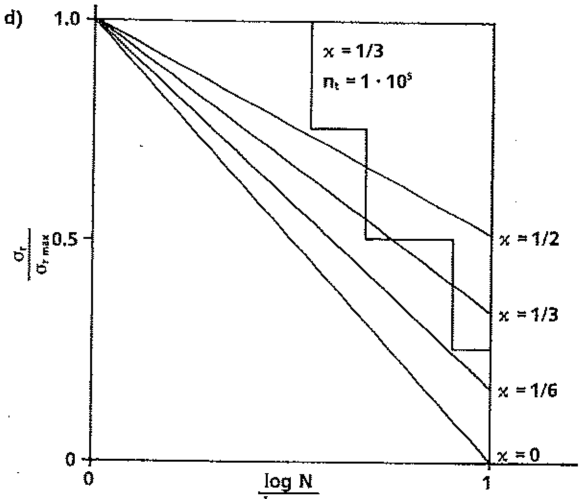

Fig. 4.6.20 *Typical example of load spectrum evaluation*

a) Carry out measurements over a number of representative working cycles. Estimate the total number of working cycles during the entire life by comparing the time taken for one working cycle and the desired life (here, $n_t = 1 \cdot 10^5$).

b) Select a number of σ_r levels on the basis of the measured load spectrum (σ_{ri} = 100, 200, 300 and 400 N/mm²).
Count the number of load cycles n_i which exceed σ_{ri} by going through the spectrum for each σ_{ri}.

c) Multiply the n_i values by the ratio between the life n_t and the total number of cycles included in the measurement ($n_i \frac{n_t}{n_1}$).
The 100 cycles with the highest σ_r are ignored provided that they are ⩽ f_{yd}. σ_{ri} = 100 N/mm² is assumed here to be equal to the fatigue limit for $n_t = 10^8$, $\varkappa$ = 1, and therefore lower levels of σ_r have not been included.

d) Plot $\sigma_r/\sigma_{r\,max}$ against log N/log n_t. Determine the value of $\varkappa$. Take very good care that the curve is a good fit at high load cycle numbers. In this example $\varkappa$ = 1/3.

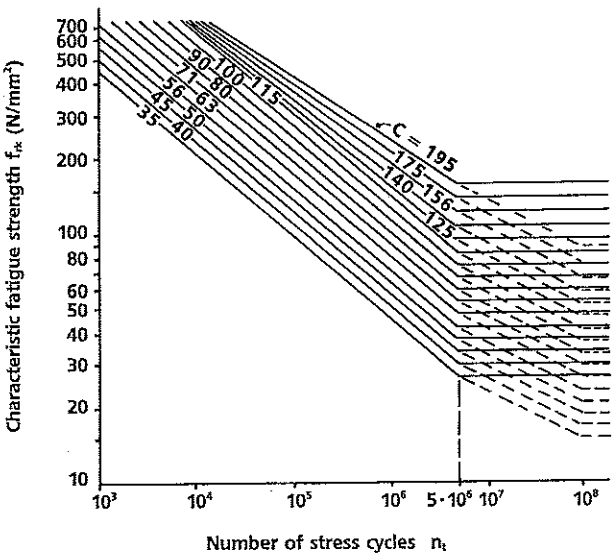

Fig. 4.6.21 *Characteristic fatigue strength f_{rk}. The full lines are used for stress spectra of constant stress range ($\varkappa$ = 1) and when fully satisfactory corrosion protection is applied. The dashed lines refer to the case when there is corrosion and, regardless of the corrosion aspect, when the cumulative damage hypothesis is applied*

On the basis of C, n_t and $\varkappa$, the characteristic fatigue strength for a constant or variable stress range can be determined from Fig. 4.6.24.

3.1 Thickness factor φ_t

The effect of sheet thickness on fatigue strength is given by

$$f_{rk} = f_{rk_0}\left(\frac{t_0}{t}\right)^{\alpha} \qquad (4.6.7)$$

Tests on offshore structures give $\alpha \sim 0.25$ for fillet welded joints. Our preliminary results indicate the following:

$\alpha \approx 0.15$ fillet welds

$\alpha \approx 0.10$ butt welds, double V welds

t_0 has been chosen to 15 mm.

The effect of thickness is taken into consideration here by multiplying f_{rk} by the thickness factor φ_t in accordance with Fig. 4.6.22. For thicknesses below 15 mm it is always conservative to put $\varphi_t = 1$. For unwelded material and spot welds, put $\varphi_t = 1$.

3.2 Material factor φ_m

For parent material the fatigue strength increases with increasing static strength if the material is unaffected by welding or thermal cutting, Fig 4.6.23 (Ref. 4:38). (The distance from the edge of the weld or the cut must be at least 3t or at least 50 mm). Sheared or punched

Thickness	φ_t	
t, mm	Butt weld Double V weld	Fillet weld
1–4	1.14	1.22
5	1.12	1.18
6	1.10	1.14
7	1.08	1.12
8	1.06	1.10
9	1.05	1.08
10	1.04	1.06
11	1.03	1.05
12	1.02	1.03
13	1.015	1.02
14	1.01	1.01
15	1.00	1.00
16	0.99	0.99

Fig. 4.6.22 *The thickness factor φ_t*

surfaces may have microcracks which eliminate the material effect (Ref. 4:39). Punch burrs in thin cold rolled sheet (t ⩽ 1 mm) do not however produce this effect.

For weld affected material $\varphi_m = 1$.

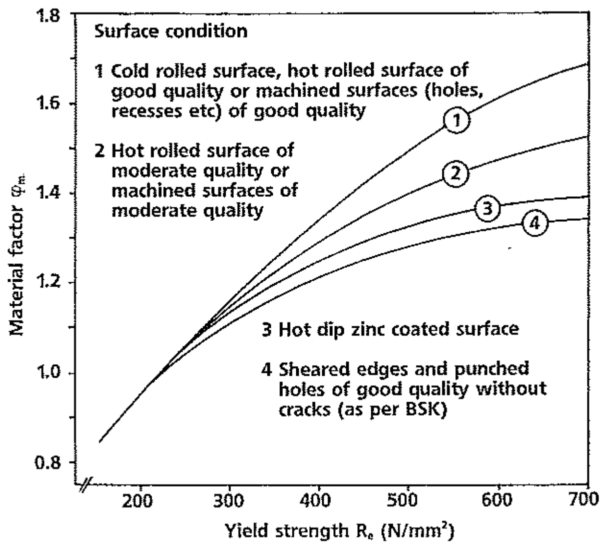

Fig. 4.6.23 *Material factor φ_m (Ref. 4:35, 38, 39)*

3.3 Stress alternation factor φ_e

If the magnitude of residual stresses is known in the region affected by the stress raiser, f_{rk} may be multiplied by φ_e:

$$\varphi_e = \frac{1 - R}{1 - 0.7\,R} \quad (R < 0) \qquad (4.6.8)$$

where $R = \sigma_{min}/\sigma_{max}$ is the local value of R with respect to the residual stresses. If σ_{max} is also a compressive stress, put $\varphi_e = 1.43$.

With regard to the effect of mean stress (R value) and the residual stresses, parent material is treated in the calculations in the same way as material affected by welding.

4 Risk of failure, partial factors of safety γ_{mn} and γ_f

Depending on the consequences of failure, the partial safety factor for design capacity, $\gamma_{mn} = \gamma_m \gamma_n$, is selected in accordance with Fig. 4.6.25. In BSK the characteristic design capacity is formally equivalent to a survival probability of 98% (mean value − 2 standard deviations). In accordance with the design practice which was applied when the engineering industry was using StBK-N2, the risk of failure is assessed in accordance with Fig. 4.6.25 (Ref. 4:40).

Consequences of failure	γ_{mn}*	Approximate risk of failure
Negligible	1.0	10^{-2}
Not very serious	1.1	10^{-3}
Serious	1.21	10^{-4}
Very serious	1.32	10^{-5}

* Since γ_m is always = 1.1 in fatigue, γ_{mn} = 1.1 γ_n.

Fig. 4.6.25 *Partial safety factor γ_{mn}*

The joint classes C are arranged as a geometric series with the ratio approximately equal to 10/9. The scatter of the Wöhler curve is usually $S_{\log \sigma r} = 0.05 - 0.06$, i.e. $S_{\log N} = 0.15 - 0.18$ for m = 3. An alteration of the joint class C by one step, for instance due to the choice of a higher Weld Quality Level, then implies a change in the risk of failure by about one order of magnitude in the failure risk region $10^{-2} - 10^{-5}$. The failure risks 10^{-1} and 0.5 are represented by γ_{mn} values of 0.88 and 0.75 respectively. This can be made use of for approximate determination of the joint class C from test results by multiplying the mean value of the fatigue strength at $2 \cdot 10^6$ cycles by 0.75.

If the joint classes according to BSK are compared with internationally recommended values (Ref. 4:41), the latter are consistently about one step higher. This implies that BSK confers about 10% extra safety.

The design stress range is

$$\sigma_{rd} = \gamma_f \, \sigma_r \qquad (4.6.9)$$

Maximum or characteristic loads are usually employed in design, and γ_f can be put equal to 1.0.

However, if the mean value of the load is used, a load factor $\gamma_f = 1.1 - 1.2$ should be applied depending on the magnitude of the scatter.

5 Design criterion

$$\sigma_{rd} \leqslant f_{rd} \qquad (4.6.10)$$

i.e.

$$\sigma_r \, \gamma_f \leqslant \frac{f_{rk} \, \varphi_t \, \varphi_m \, \varphi_e}{\gamma_{mn}} \qquad (4.6.11)$$

If the stress range comprises only shear stresses, the design criterion is

$$\tau_{rd} \leqslant f_{rvd} \qquad (4.6.12)$$

where $f_{rvd} = 0.6 \, f_{rd}$, with f_{rd} as above. For bolts in Strength Classes 8.8 and 10.9, $f_{rvd} = 0.9 \, f_{rd}$.

In a multiaxial state of stress, with stress ranges $\sigma_{r//}$, $\tau_{r//}$, $\sigma_{r\perp}$ and $\tau_{r\perp}$, the following formula also applies in addition to Formulae 4.6.10 and 4.6.12.

$$\sqrt{\frac{\sigma^2_{rd//}}{f^2_{rd//}} + \frac{\sigma^2_{rd\perp}}{f^2_{rd\perp}} + \frac{\tau^2_{rd//}}{f^2_{rvd}} + \frac{\tau^2_{rd\perp}}{f^2_{rvd}}} \leqslant 1.10 \qquad (4.6.13)$$

For some types of detail in Fig. 4.6.27, Case 26 Section a − a, and Cases 43 − 50, the multiaxial state of stress has been taken into account in determining the value of C. In these cases there is no need for the condition in Formula 4.6.13 to be complied with.

Design in accordance with the Palmgren-Miner rule

The cumulative damage hypothesis for a variable stress range can be applied directly as follows if the calculation principles set out above are observed.

1. Determine a notional "stress range" $\sigma'_{ri} = \sigma_{ri}\gamma_f\gamma_{mn}/(\varphi_t\varphi_m\varphi_e)$ for each stress level σ_{ri}.
2. Ignore the 100 highest values of σ'_{ri} and the values which are below the fatigue limit at $n_t = 10^8$ cycles.
3. Apply the design criterion

$$\Sigma \left(\frac{n_i}{n_{ti}} \right) \leqslant 1.0 \qquad (4.6.14)$$

where n_i = number of stress cycles of stress range σ_{ri}
n_{ti} = life at constant "stress range" σ'_{ri}.
The life is determined from Fig. 4.6.21 by putting f_{rk} equal to σ'_{ri}.

Instead of referring to Fig. 4.6.21, n_{ti} can be determined from

$$n_{ti} = \left(\frac{C}{\sigma'_{ri}} \right)^m 2 \cdot 10^6 \qquad n_{ti} \leq 5 \cdot 10^6 \qquad (4.6.15)$$

$$n_{ti} = \left(\frac{0.4^{\left(\frac{1}{m} - \frac{1}{5}\right)} C}{\sigma'_{ri}} \right)^5 2 \cdot 10^6 \qquad 5 \cdot 10^6 < n_{ti} < 10^8 \qquad (4.6.16)$$

		Joint class C															
x	n_t	35	40	45	50	56	63	71	80	90	100	112	125	140	156	175	195
1	10^3	441	504	567	630	706	794	895	1010	1130	1260	1410	1410	1410	1410	1410	1410
	10^4	205	234	263	292	327	368	415	468	526	585	655	677	701	724	750	775
	10^5	95.0	109	122	136	152	171	193	217	244	271	304	325	348	372	398	425
	10^6	44.1	50.4	56.7	63.0	70.6	79.4	89.5	101	113	126	141	156	173	191	212	234
	$5 \cdot 10^6$	25.8	29.5	33.2	36.8	41.3	46.4	52.3	58.9	66.3	73.7	82.5	93.3	106	120	136	154
5/6	10^3	515	588	661	735	823	925	1040	1180	1320	1470	1650	1650	1650	1650	1650	1650
	10^4	241	275	309	343	384	433	487	549	618	687	769	796	824	851	881	911
	10^5	112	128	144	160	179	202	227	256	288	320	358	384	411	439	471	502
	10^6	52.3	59.8	67.1	74.5	83.4	93.9	106	119	134	149	167	185	205	226	251	277
	10^7	26.7	30.5	34.2	38.0	42.6	47.9	54.0	60.8	68.4	76.0	85.1	96.6	110	124	141	159
	10^8	16.9	19.3	21.6	24.0	26.9	30.3	34.1	38.4	43.2	48.0	53.8	61.1	69.3	78.2	89.0	100
2/3	10^3	615	703	790	878	983	1110	1250	1400	1580	1760	1970	1970	1970	1970	1970	1970
	10^4	291	333	373	415	465	523	589	664	747	830	929	962	995	1030	1060	1100
	10^5	137	156	175	195	218	245	277	312	351	390	436	467	500	534	572	611
	10^6	63.9	73.1	82.0	91.1	102	115	129	146	164	182	204	226	250	276	307	338
	10^7	32.7	37.4	41.9	46.6	52.2	58.7	66.1	74.5	83.8	93.1	104	118	134	152	173	195
	10^8	20.7	23.7	26.6	29.5	33.0	37.2	41.9	47.2	53.1	59.0	66.1	75.1	85.2	96.2	109	123
1/2	10^3	759	867	976	1080	1210	1370	1540	1740	1950	2170	2430	2430	2430	2430	2430	2430
	10^4	366	418	470	522	585	658	742	836	940	1040	1170	1210	1251	1290	1340	1380
	10^5	174	199	223	248	278	313	352	397	447	496	556	595	637	679	728	776
	10^6	82.0	93.7	105	117	131	147	166	187	210	234	262	290	321	354	393	433
	10^7	42.2	48.3	54.0	60.0	67.2	75.6	85.2	96.0	108	120	134	153	173	196	222	251
	10^8	26.9	30.7	35.2	39.1	43.8	49.2	55.5	62.5	70.3	78.1	87.5	97.2	110	125	142	160
1/3	10^3	975	1110	1260	1400	1560	1760	1980	2230	2510	2790	3130	3130	3130	3130	3130	3130
	10^4	489	558	627	697	781	878	990	1120	1250	1390	1560	1610	1660	1710	1760	1810
	10^5	238	272	305	339	380	427	481	542	610	678	759	811	867	924	988	1050
	10^6	114	130	146	162	182	205	230	260	292	325	364	402	445	490	543	598
	10^7	59.3	67.8	75.7	84.1	94.2	106	119	135	151	168	188	214	243	274	311	351
	10^8	38.1	43.5	51.3	57.0	63.9	71.9	81.0	91.3	103	114	128	138	156	176	200	225
1/6	10^3	1300	1480	1680	1870	2090	2350	2650	2990	3360	3740	4100	4100	4100	4100	4100	4100
	10^4	703	804	904	1000	1130	1270	1430	1610	1810	2010	2250	2300	2360	2410	2460	2500
	10^5	362	414	465	516	578	651	733	826	929	1030	1160	1230	1300	1380	1460	1540
	10^6	181	207	232	258	289	325	366	412	464	515	577	635	700	766	843	921
	10^7	97.1	111	123	137	153	173	194	219	246	274	307	350	395	443	501	561
	10^8	63.9	73.0	81.9	91.0	102	115	129	146	164	182	204	230	260	292	331	371
0	10^3	1700	1940	2220	2470	2760	3110	3500	3950	4440	4940	5200	5200	5200	5200	5200	5200
	10^4	1040	1190	1340	1490	1670	1880	2120	2390	2680	2980	3340	3340	3350	3360	3360	3360
	10^5	603	689	775	861	964	1080	1220	1380	1550	1720	1930	2000	2080	2150	2220	2280
	10^6	336	384	432	481	538	605	682	769	865	961	1090	1150	1238	1320	1410	1500
	10^7	186	213	241	267	299	337	380	428	481	535	599	654	720	790	870	940
	10^8	112	128	144	160	179	202	227	256	288	320	359	395	433	480	530	570

Fig. 4.6.24 *Characteristic fatigue strength f_{rk} (N/mm^2) for standardized stress spectra (Ref. 4:1)*

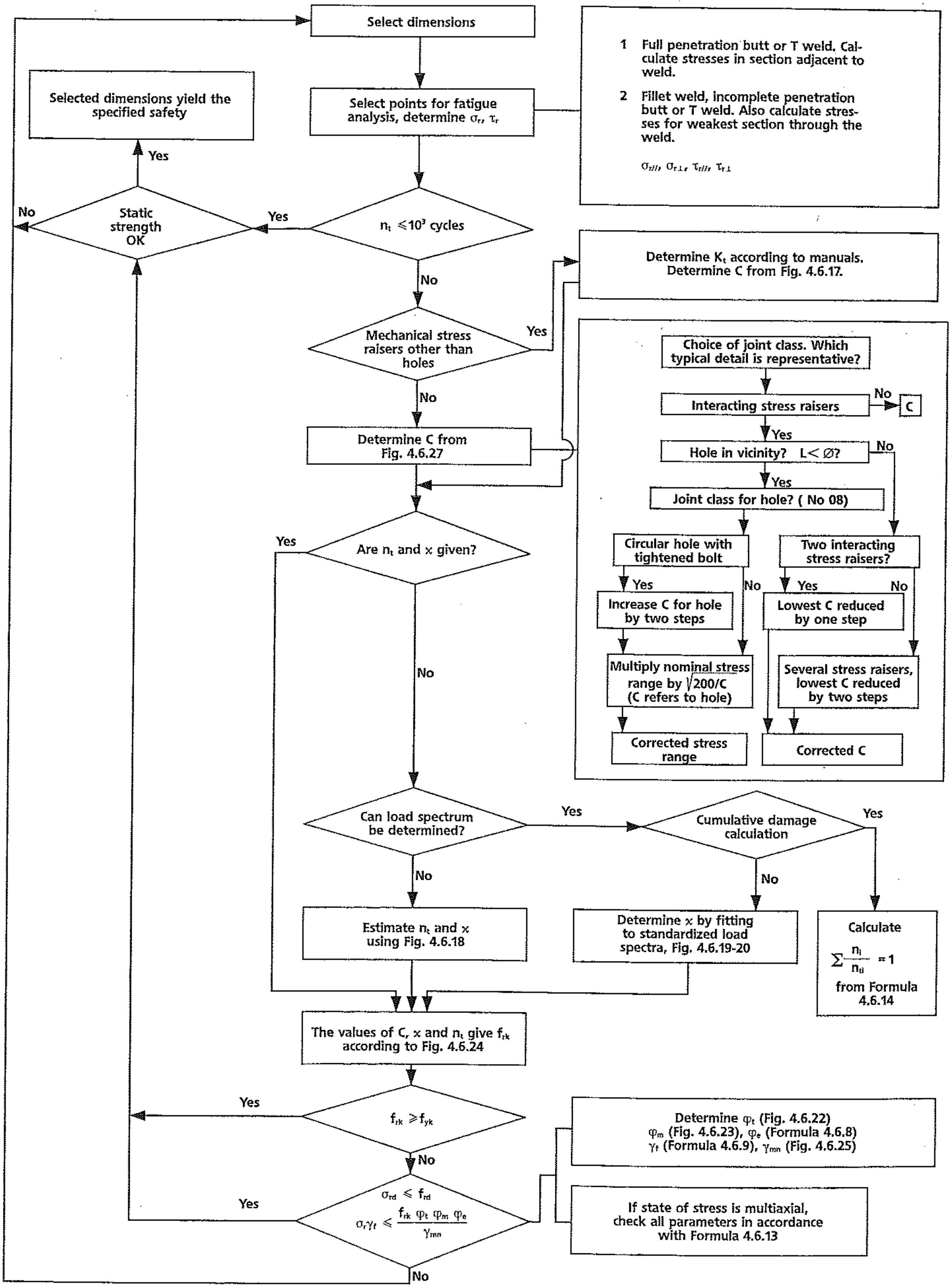

Fig. 4.6.26 *Calculation procedure in fatigue design*

FIG. 4.6.27a) *Joint classes C for parent material and welded joints (Ref. 4:1). The weld quality levels given are defined in Swedish Standard SS 06 61 01. Weld Quality Levels WB and WC correspond approximately to Quality Levels B and C in accordance with ISO/DIS 5817.3, while WA denotes a higher quality level.*

In the figures, --- marks the regions affected by the stress concentration factor for which the values of C given apply. The arrows indicate the *direction* of the stress and not the type of stress (normal stress — shear stress, tension — compression).

a Where the root of the weld is not given a sealing run, the value of C shall be reduced by one step for $C_{//}$ and by two steps for $C_{\perp}$ in the series of values of C (35, 40, 45, 50, 56, 63, 71, 80, 90, 100, 112, 125, 140, 156, 175 and 195, see FIG. 4.6.21).

b The joint is capable of transmitting shear force.

No	Joint configuration		C	Remarks
01	Parent material, ground surface		215	
02	Parent material, rolled surface		175 156 140	Good quality Moderate quality Exposed surface of slow rusting steel
03	Parent material, sand blasted surface			See Nos 02 and 04 – 07
04	Parent material, hot dip zinc coated surface		156	
05	Parent material, sawn surface		156 175	Workmanship Class GB Workmanship Class GA Chamfered edges
06	Parent material, sheared surface			See No 05
07	Thermally cut surface		90 112	Surface roughness < 0.3 mm Corners machined to 2 mm chamfer. Surface roughness < 0.2 mm
08	Open circular holes 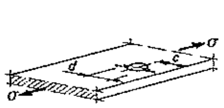	1.5d ⩽ c < 3d c ⩾ 3d	71 80	Stress range may be calculated over gross area. For reamed holes with chamfered edges, values of C may be increased by one step. For punched holes, values of C shall be reduced by one step. For values of C for bolted joints, see Fig.4.6.27 b)
09	Stud 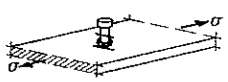		63	Mechanized flash welding with quality requirements in accordance with technical rules of Swedish National Road Administration

No	Joint configuration	Weld quality level	$C_{//}$	$C_{\perp}$	Remarks
10	Butt weld in double V joint 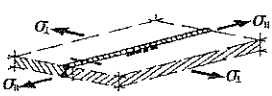	WC WB WA	80 100 112	63 90 112	
11	Butt weld in single V joint 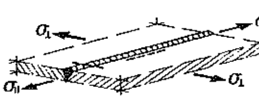	WC WB WA	80 100 112	63 90 112	With root with a sealing run, alternatively welded against a backing bar or backing strip which is removed
12	Butt weld in single V joint 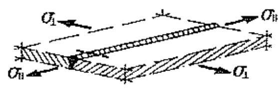	WC WB	71 90	50 71	No sealing run on root, but the quality requirement for the specified weld quality level shall apply for the root side also
13	Butt weld in single V joint with backing strip left in position 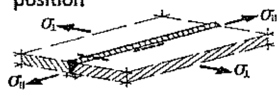	WC WB	71 90	50 56	
14	Butt weld with incomplete penetration 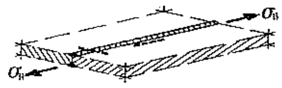	WC WB	71 90	– –	
15	Butt weld at change in sheet thickness 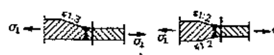	WC WB WA	71 90 100	56 71 90	Root with sealing run [a]
16	Butt weld at change in sheet thickness 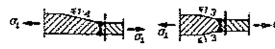	WC WB WA	80 100 112	63 80 100	Root with sealing run [a]
17	Butt weld at change in sheet width 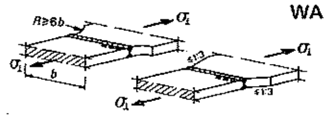	WC WB WA	– – –	63 80 100	Root with sealing run [a]
18	Butt weld at girder splice 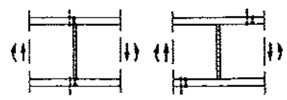	WC WB WA	– – –	63 80 100	Butt weld with sealing run [a] Rolled or welded girder. However, C value for WA applies only for welded girder. In a welded girder, other sections must also be checked, see e.g. No 30
19	Butt weld at girder splice (rolled girder) 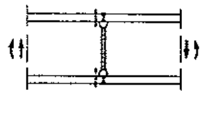	WC WB WA	– – –	63 80 90	Root with sealing run [a] Drilled or ground hole. For WA, edge of hole must also be dressed (see No 08). (See Nos 25 & 33 for welded girder)
20	Butt weld at longitudinal attachment 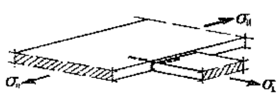	WB WA	45 50	45 50	Root with sealing run
21	Butt weld at longitudinal attachment 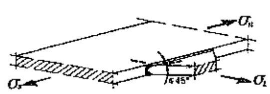	WC WB WA	50 56 71	45 50 56	Root with sealing run

Fig. 4.6.27 a) (cont)

No	Joint configuration	Weld quality level	$C_{//}$	$C_{\perp}$	Remarks
22	Double V T-butt weld 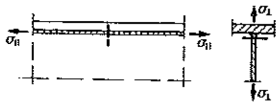	WC WB WA	80 100 112	56 71 90	
23	Single V T-butt weld 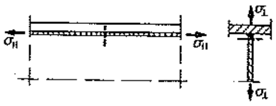	WC WB WA	71 90 100	50 63 80	Root with sealing run. Symmetrical cross section, I or box section
24	Weld with partial penetration 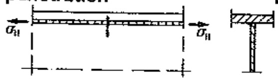	WC WB	63 71	– –	Penetration shall be equal to at least half the sheet thickness (bottom sheet in figure)
25	T-butt weld at girder splice (welded girder) 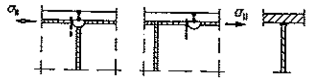	WC WB WA	63 71 80	– – –	Drilled or ground hole. Values of C apply for the ends of the T-weld
26	T-butt weld, e.g. at beam-column joint — Sect. a – a	WC WB WA	– – –	56 71 90	The force at Section b – b may be assumed dispersed over 45° as in the figure (applies also to rolled column of I section, in which case the values of $C_{\perp}$ for Section b – b may be put equal to 90)
	Sect. b – b 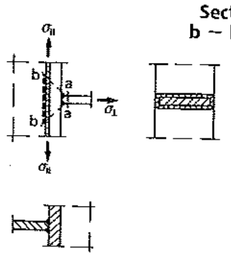	WC WB WA	80 100 112	56 71 90	
27	Continuous single V butt weld at attachment of circular or rectangular hollow section to stiff plate 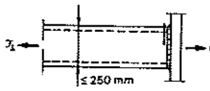	WC WB	– –	45 50	
28	T-butt weld at longitudinal attachment 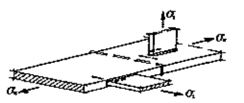	WC WB WA	– 45 50	– 45 50	
29	T-butt weld at longitudinal attachment 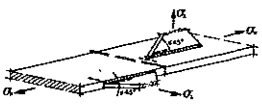	WC WB WA	50 56 71	45 50 56	
30	Fillet weld 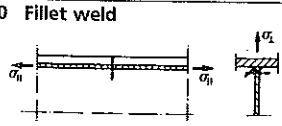	WC WB WA	71 80 100	50 56 63	Manual welding

No	Joint configuration	Weld quality level	$C_{//}$	$C_{\perp}$	Remarks
31	Fillet weld 	WC WB WA	80 90 100	50 56 63	Mechanized welding
32	Fillet weld on one side only 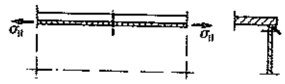	WC WB WA	63 71 80	– – –	
33	Fillet weld at girder splice 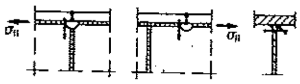	WC WB WA	56 63 80	– – –	Drilled or ground hole. Values of C apply for the ends of the fillet weld. Other sections must also be checked, see e.g. No 12
34	Intermittent fillet weld between flange and web of I girder 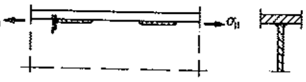	WC WB	50 56	– –	
35	Fillet weld at longitudinal attachment 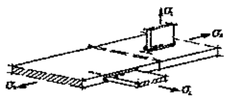	WC WB WA	– 45 50	– 45 50	Values of C given also apply to sections through the weld metal
36	Fillet weld at longitudinal attachment 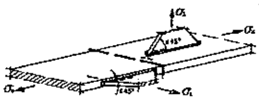	WC WB WA	50 56 71	45 50 56	Values of C given also apply to sections through the weld metal

No	Joint configuration	Weld ...	C	Remarks
37	Fillet welded longitudinal cleat [b] 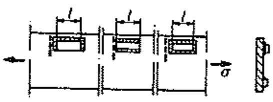	WC WB WA	45 50 63	When L ⩽ 100 mm, the values of C may be increased by one step
38	Fillet welded transverse cleat [b] 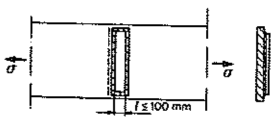	WC WB WA	45 50 63	If the width of the cleat is less than half the sheet width values of C may be increased by one step. If L ⩾ 100 mm, No 48 shall be applied
39	Fillet weld at transverse attachment [b] 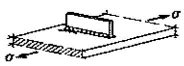	WC WB WA	45 56 80	Weld not returned at the ends. The values of C given may also be applied to T-butt welds
40	Fillet weld at transverse attachment [b] 	WC WB WA	45 63 90	Weld returned at the ends. The values of C given may also be applied to T-butt welds
41	Fillet weld at longitudinal attachment [b] 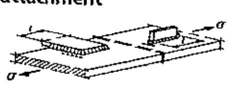	WC WB WA	45 50 63	When L ⩽ 100 mm, values of C may be increased by one step. The weld is not designed for transmission of force

Fig. 4.6.27 a) (cont)

No	Joint configuration	Weld quality level	C	Remarks
42	Intermittent fillet weld between crane rail and crane girder 	WC WB	50 56	Good contact between rail and top flange
43	Continuous beam with stiffeners over intermediate support (the figure shows three alternatives) 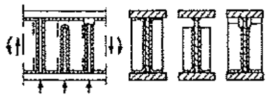	WC WB WA	50 63 80	The stress range is to be calculated at the edge of the stiffener. Weld returned at the ends
44	Beam with web stiffeners in the span and above outer supports (cp No 43) 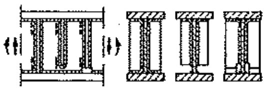	WC WB WA	56 71 90	The stress range is to be calculated at the edge of the stiffener. Weld is returned at the ends. The values of C also apply for single stiffeners
45	Box girder with stiffeners 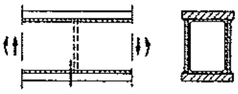	WC WB WA	56 63 71	Weld returned at the ends. The values of C also apply for single stiffeners
46	Beam with longitudinal web stiffeners 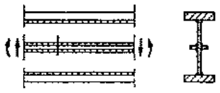	WC WB WA	63 71 90	Manual welding
47	Beam with longitudinal web stiffeners 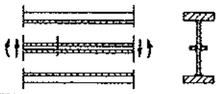	WC WB WA	71 80 90	Mechanized welding
48	Beam with cover plate 	WC WB WA	– 45 50	With or without transverse fillet weld for WB. For WA, the transverse fillet weld and at least 100 mm of the longitudinal fillet welds nearest the corner shall be dressed
49	Beam with cover plate 	WC WB WA	– 45 50	With transverse fillet weld. For WA, the transverse fillet weld and at least 100 mm of the longitudinal fillet welds nearest the corner shall be dressed
50	Beam with cover plate 	WA	63	Transverse fillet weld shall be dressed to slope of 1:3 or less. At least 100 mm of longitudinal fillet welds nearest the corner shall be dressed to Quality Level WA
51	Beam with cover plate 	WC WB WA	80 90 100	Relates to section at least one flange width distant from end of cover plate

No	Joint configuration	Weld quality level	C	Remarks
52	Fillet welded attachment of member 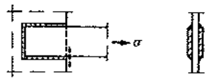	WC WB WA	45 50 56	
53	Fillet welded attachment of member 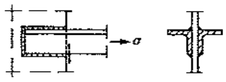	WC WB WA	– 45 50	
54	Fillet welded symmetrical lap joint 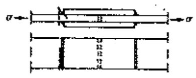	WC WB WA	50 56 63	
55	Fillet welded symmetrical lap joint 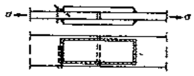	WC WB WA	45 50 56	
56	Continuous single fillet weld at attachment of circular or rectangular hollow section to stiff plate 	WC WB WA	– 45 50	
57	Spot weld 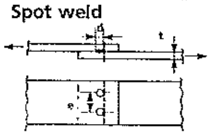	WB	50	$F_{rk} = \dfrac{3 f_{rk}\, t}{\dfrac{2}{\pi d} + \dfrac{3}{e}}$
58	Spot welded hat section 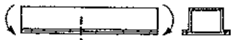	WB	112	
59	Box section with non load-carrying spot welds 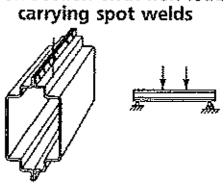	WB	125	
60	Box section with load-carrying spot welds 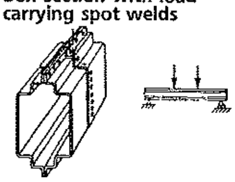	WB	60	
61	Plug weld 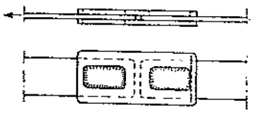	WC WB WA	71 90 100	

Fig. 4.6.27 b) *Joint class C for joints comprizing fasteners (Ref. 4:1)*

Joint configurations Nos 01 to 12 relate to parent material with drilled or reamed holes. For punched holes the values of C shall be reduced by one step. Threaded holes are not dealt with. The arrows indicate the *direction* of stress, not the type of stress (bending stress—normal stress etc).

No	Joint configuration	C	Remarks
01	Splice or attachment of flat bar by means of a double shear joint 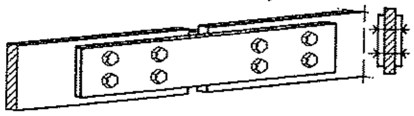	100	
02	Splice or attachment of flat bar by means of a single shear joint 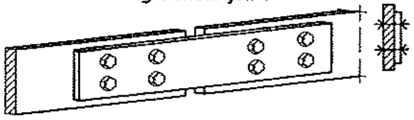	50	
03	Splice or attachment of each part a member by means of a double shear joint 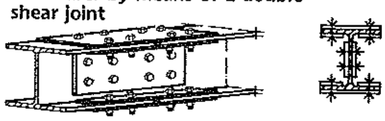	90	
04	Splice or attachment by means of a partly double shear joint 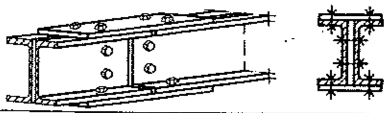	71	Axial force in member
05	Splice or attachment of part of a member by means of a double shear joint 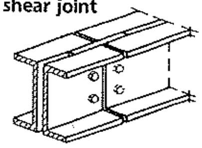	71	Axial force in member
06	Splice or attachment by means of a single shear joint 	71	Axial force in member
07	Splice or attachment by means of single shear joints 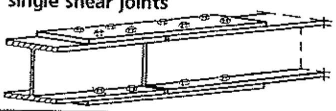	63	Axial force in member
08	Unsymmetrical splice or attachment by means of a single shear joint 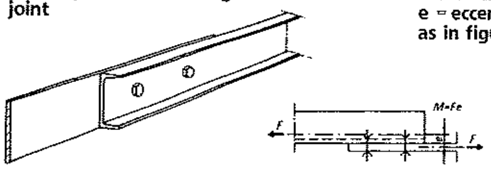	50 45	For $e \leqslant 2t$ For $e > 2t$ e = eccentricity as in figure
09	Cover plate with single shear joint 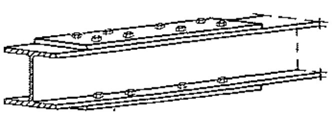	63	Relates to section within one flange width from the end of the cover plate
10	Cover plate with single shear joint For figure, see No 09	80	Relates to section at least one flange width from the end of the cover plate
11	Flange brace attached by single shear joint 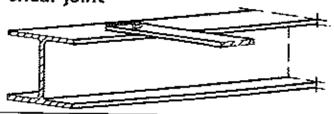	80	Relates to the effect of the hole in the beam for a normally tightened bolt. For design of bracing, see 02
12	Attachment of member to gusset plate by double shear joint 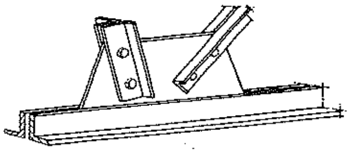	71	
13	Fastener, acted upon by shear force, in single shear joint 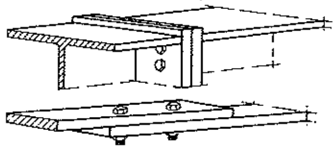	90	Value of C applies for close tolerance joints
14	Fastener, acted upon by shear force, in multishear joint 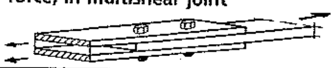	112	Value of C applies for close tolerance joints
15	Fastener acted upon by tensile force 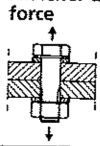	45	Value of C applies for a tightened bolt in Strength Class 8.8 or higher. For a non-tightened bolt, No 16 applies
16	Threaded constructional element 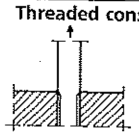	<45 See remark	The design value f_{rd} for a rolled thread is 90%, and for a cut thread 70%, of the value for Joint Class 45

4.7 Defect tolerance

Regardless of how much effort is made to produce "perfect" structures, it is impossible, especially in welded structures, to avoid defects completely. This section describes the way in which the effect of different defects on the design capacity or life can be analysed by fracture mechanics. Examples of questions which can be answered by fracture mechanics are

- Will a defect grow under the applied fatigue loading?
- What size of defect is critical with regard to the risk of brittle failure?
- How many load cycles are required for the defect to attain a critical size?

4.7.1 Fracture mechanisms

Different types of fracture occur under different geometrical and loading conditions and as a result of material characteristics. The types of fracture can be broadly classified as

- Brittle fracture
- Ductile fracture
- Fatigue fracture

Brittle fracture is characterized by the fact that fracture is accompanied by plastic strain which is negligible on a macroscopic scale and that fracture progresses very rapidly through the material. On the fracture surfaces there is often a chevron pattern which points towards the point of initiation.

Ductile fracture is accompanied by considerable plastic strain. The fracture surfaces cannot be fitted together after fracture, and the velocity of propagation is much lower than in the case of brittle fracture.

Fatigue fracture occurs when a crack or defect grows to a critical size under the action of fatigue loading. The actual crack growth takes place in a large number of small increments (10^{-2} – 10^{-6} mm/load cycle) and in most cases without visible plastic strain. The plastic flow which does occur is very local at the point of the crack tip and can sometimes be seen as striations in an electron microscope. On the other hand, the oystershell shaped pattern of lines which can be seen by the naked eye consists of arrest lines which are formed when the crack front is stationary or the load is changed.

Final fracture after fatigue crack propagation may be brittle or ductile.

4.7.2 Fundamental fracture mechanics

Fracture mechanics is treated more in detail in e.g. Ref. 4:42 – 44.

From the standpoint of the user, fracture mechanics may be divided into determination of the critical crack size with respect to static failure and an analysis of crack propagation under fatigue loading.

Critical crack size

Brittle fracture

There is a risk of brittle fracture if the following three conditions are satisfied:

- A sufficiently high stress in the construction
- A sufficiently low temperature
- A sufficiently high degree of triaxial stress

A triaxial state of stress often requires large plate thicknesses, and for this reason brittle fracture seldom occurs in materials less than 16 mm thick, which is the upper limit for SSAB Strip products.

The critical crack size with regard to brittle fracture is determined by linear fracture mechanics. The severity of the stress field in the vicinity of the crack tip is measured by the *stress intensity factor K*. In the loading case of the greatest practical interest, load direction perpendicular to the crack, Mode I, the stress intensity factor K_I is given by

$$K_I = \sigma\sqrt{\pi a}\, f \qquad (4.7.1)$$

where σ = nominal stress (disregarding the crack) plus residual stresses if any
a = crack depth, Fig. 4.7.1
f = geometry function which allows for the effect of the shape of the crack and the component concerned and for the type of load (tension or bending). See also subsection 4.7.3.

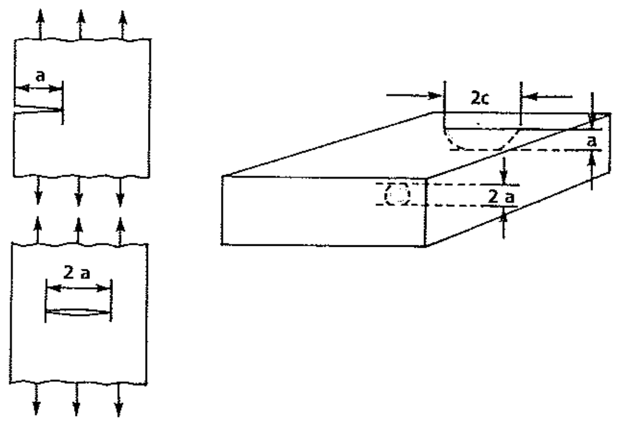

Fig. 4.7.1 *Definition of crack depth*

Fracture occurs when

$$K_I = K_{IC} \qquad (4.7.2)$$

where K_{IC} = fracture toughness of material. Note that the fracture toughness has the dimensions $MNm^{-3/2}$ (= MPa $\sqrt{m}$)

When a safety factor is introduced, for instance in Formula 4.7.1, it should be noted that a factor of 2 on the stress is equivalent to a factor of 4 on the crack depth.

The fracture toughness is a material property, but in order that valid values should be obtained in tests, it is necessary for the conditions relating to linear fracture mechanics to be satisfied:

$$\left.\begin{matrix} t \\ a \end{matrix}\right\} \geq 2.5\left(\frac{K_{IC}}{R_e}\right)^2 \qquad (4.7.3)$$

The fracture toughness, which decreases as temperature drops, is determined in standardized tests.

Fracture toughness must not be confused with Charpy impact strength (KV). Impact strength is used as a qualitative measure of the ductility of the material but cannot be used for direct calculation of critical defect sizes. There is however an approximate relationship between impact strength and fracture toughness; see subsection 4.7.3.

If only the crack length requirement in Formula 4.7.3 is satisfied, the failure condition 4.7.2 can be replaced by

$$K_I = K_C \qquad (4.7.4)$$

where K_C is the toughness of the material at the thickness concerned. In this case tests are carried out on material of the same thickness as that in the structure, since toughness varies with thickness, Fig. 4.7.2.

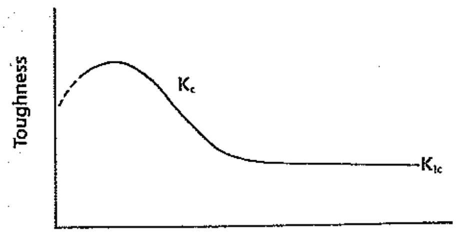

Fig. 4.7.2 Typical relationship between toughness and sheet thickness

Ductile fracture

When the conditions for linear fracture mechanics are not satisfied, nonlinear fracture mechanics are applied. An engineering method which is particularly useful for welded joints is the CTOD (Crack Tip Opening Displacement) method. This is based on the fact that the toughness of a material can be defined by the opening of the crack tip which can occur before fracture is initiated. Toughness is given in terms of critical CTOD which is usually denoted δ_c and has the dimension length. Typical values of δ_c for welded joints are 0.1 – 0.3 mm.

The total strain, i.e. nominal strain plus strain due to residual stresses, is used as a measure of the load. For this reason, welds with strains greater than the yield strain can for instance be treated; see also Ref. 4:45.

Crack growth under fatigue loading

In conjunction with fatigue loading, the crack driving parameter is the stress intensity range ΔK_I.

$$\Delta K_I = \Delta\sigma\sqrt{\pi a}\, f \qquad (4.7.5)$$

where $\Delta\sigma = \sigma_{max} - \sigma_{min}$ for welded joints where the residual stresses have not been eliminated, or if $\sigma_{min} > 0$

$\Delta\sigma = \sigma_{max}$ in other cases

The relationship between the crack driving parameter ΔK (the subscript I is often omitted in a fatigue context) and da/dN (crack growth per load cycle) is plotted in Fig. 4.7.3. The figure has three regions. In the left hand region where the values of ΔK are lowest (threshold region) the curve deflects downwards, and below $\Delta K = \Delta K_{th}$ (threshold value) there is no crack growth. In the linear intermediate region the relationship between da/dN and ΔK can be described by the Paris law

$$da/dN = C\,\Delta K^n \qquad (4.7.6)$$

For values of ΔK above the Paris region K_{max} approaches the toughness of the material (K_{IC}, K_C), and the rate of crack growth increases very rapidly as the value of ΔK increases (instability region).

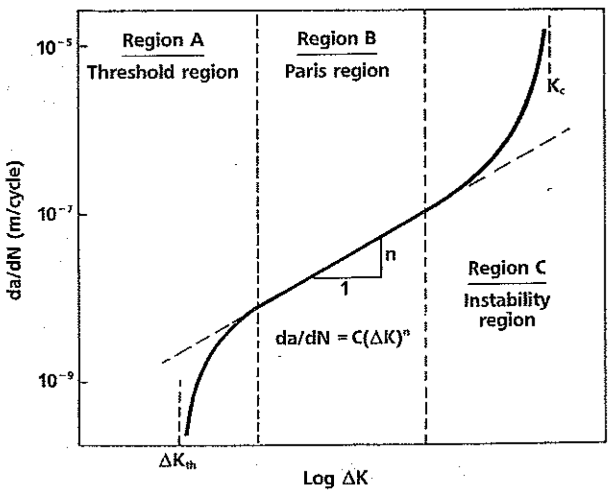

Fig. 4.7.3 Relationship between rate of crack growth and stress intensity variation (Ref. 4:43)

4.7.3 Data for fracture mechanics calculations

Fracture mechanics calculations require knowledge of material data (K_{IC}, K_C, K_{th}, C, n), the geometry factor (f) in the expression for the stress intensity factor, and the depth of any defects or cracks which may be present.

Threshold value for crack propagation, ΔK_{th}

The threshold value is mainly dependent on the microstructure of the steel and on the loading conditions R. If the threshold value for the material in question is not known, the following expression which yields conservative values for steels can be used for R (= $\sigma_{min}/\sigma_{max}$) > 0 (Ref. 4:29)

$$\Delta K_{th} = 6 - 4.5\,R \quad (MNm^{-3/2}) \qquad (4.7.7)$$

but at least 2 $MNm^{-3/2}$

R relates to the local loading condition in the vicinity of the crack, i.e. it includes any residual stresses which may be present. If these are not known, they should when welded joints are analysed be assumed to be at the level of the yield stress. The R ratio is then

$$R = (R_e - \Delta\sigma)/R_e$$

Short cracks, $a < 0.5 - 1$ mm, can grow at values of ΔK_{th} lower than those given by Formula 4.7.7. In such cases, use $\Delta K_{th} = 2\ MNm^{-3/2}$ or correct the crack length in accordance with Ref. 4:44.

Fracture toughness K_{Ic} or K_c

For structural steels, fracture toughness is usually within the range $50 < K_{Ic} < 250\ MNm^{-3/2}$. Fig. 4.7.4 sets out the values of fracture toughness for some steels.

Fig. 4.7.4 *Values of fracture toughness*

Material	Thickness (mm)	Temperature (°C)	K_c ($MNm^{-3/2}$)
S275JR	20	−20	210
DOMEX 355W	10	−20	175
WELDOX 420	19.5	−40	141
WELDOX 420	40	−60	150
DOMEX 024 B*	8	0	62
DOMEX 024 B*	8	−20	55
DOMEX 024 B*	8	−40	48
DOMEX 024 B**	8	0	72
DOMEX 024 B**	8	−20	42
DOMEX 024 B**	8	−40	63
DOMEX 044 B*	8	0	77
DOMEX 044 B*	8	−20	72
DOMEX 044 B*	8	−40	62
DOMEX 044 B**	8	0	62
DOMEX 044 B**	8	−20	61
DOMEX 044 B**	8	−40	59
S275JR G3	25	−20	210
S355JR	25	−40	90
S355JR G3	20	−20	190

* Quenched in oil ** Quenched in water

If fracture toughness data are not available, the following expressions (Ref. 4:46) can give an approximation of the fracture toughness on the basis of impact strength data. See also Fig. 4.7.5.

$$\left.\begin{aligned} K_c &= 11.76\,KV^{0.66} \quad KV \leq 45\ J \\ K_c &= 54.40\,KV^{0.26} \quad KV > 45\ J \end{aligned}\right\} \qquad (4.7.8)$$

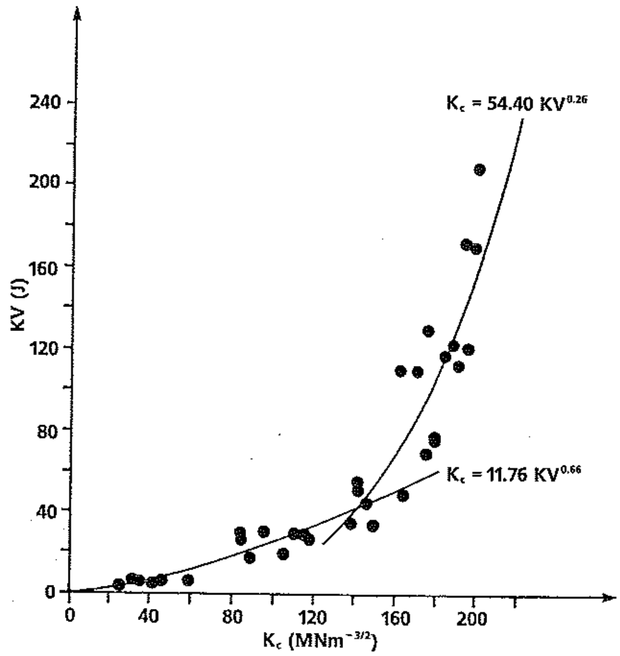

Fig. 4.7.5 *Fracture toughness as a function of impact strength (Ref. 4:46)*

Crack propagation constants C and n

In the linear Paris region crack growth is less dependent on microstructure and the R ratio than in the threshold and instability regions. This means that the same crack propagation data can be used for both parent material and weld metal.

There is a high degree of correlation between C and n (Ref. 4:47). If, for instance, the values of C in Fig. 4.7.6 are recalculated for n = 3 and if it is assumed that the scatter is the same as that obtained in Ref. 4:29, the following values of C (ΔK in $MNm^{-3/2}$ and da/dN in m per cycle) are obtained:

$$\left.\begin{aligned} C &= 3.9 \cdot 10^{-12} \quad \text{(mean value, 50th percentile)} \\ C &= 12.2 \cdot 10^{-12} \quad \text{(95th percentile)} \\ C &= 23.4 \cdot 10^{-12} \quad \text{(99.5th percentile)} \\ n &= 3 \end{aligned}\right\} \qquad (4.7.9)$$

C is dependent on the units in which calculation is carried out:

$$\log C_1 = \log C_2 + 1.5\,n - 3 \qquad (4.7.10)$$

where C_1 applies when the crack length is in m and the stress intensity factor in $MNm^{-3/2}$
C_2 applies when the crack length is in mm and the stress intensity factor in $Nmm^{-3/2}$

Material	$C\ (10^{-12})$			n
	Mean value	Percentile		
		95th	99.5th	
DOCOL 350	0.98	1.3	1.6	3.34
DOCOL 500 YP	0.70	0.95	1.1	3.39
DOCOL 800	5.3	6.9	8.0	2.82
DOMEX 355 YP	0.56	–	–	3.42
DOMEX 355 YP	3.8	–	–	2.98
DOMEX 355 YP	5.2	–	–	2.89
DOMEX 355 YP	29	–	–	2.39
DC04	0.091	0.14	0.18	4.19
S235JR	0.020	–	–	3.31
S355N	0.85	–	–	3.33
SS 2142	2.4	–	–	3.14

Fig. 4.7.6 *Examples of C and n values for some of the products of SSAB Strip Products. da/dN in m/cycle and ΔK in $MNm^{-3/2}$*

Geometry factor f

The geometry factor f is often broken down into a number of partial factors, each of which takes account of a special geometrical effect. The principle of subdivision is set out in Ref. 4:44.

If the distance between the crack front and the external surface of the body "in front" of the crack is considerably larger than a, the value of f for cracks in a *material without stress concentrations* can be approximated by the expression

$f = 1.12\ f_{10}$ for surface cracks (4.7.11 a)

$f = f_{10}$ for internal cracks (4.7.11 b)

Values of f_{10} are plotted in Fig. 4.7.7. Through cracks, the figure at the left of Fig. 4.7.1, are represented in Fig. 4.7.7 by $a/c = 0$.

For the most common fatigue cracks in *welded joints* (shallow surface cracks, $a/t < 0.2$, and long cracks, $a/c < 0.1$), sufficient accuracy is in most cases obtained when f is approximated by

$$f = 1.12\ M_k \qquad (4.7.12)$$

where M_k is a factor which corrects for the crack being situated in a region where there is an external stress concentration. M_k is a function of the degree of stress concentration K_t and the crack depth. When $a \to 0$, $M_k \to K_t$, and for a surface without macrogeometric stress concentrations $M_k = 1.00$. Generally $1 < M_k < K_t$.

When there are internal defects in welded joints, Formula 4.7.11b can be used.

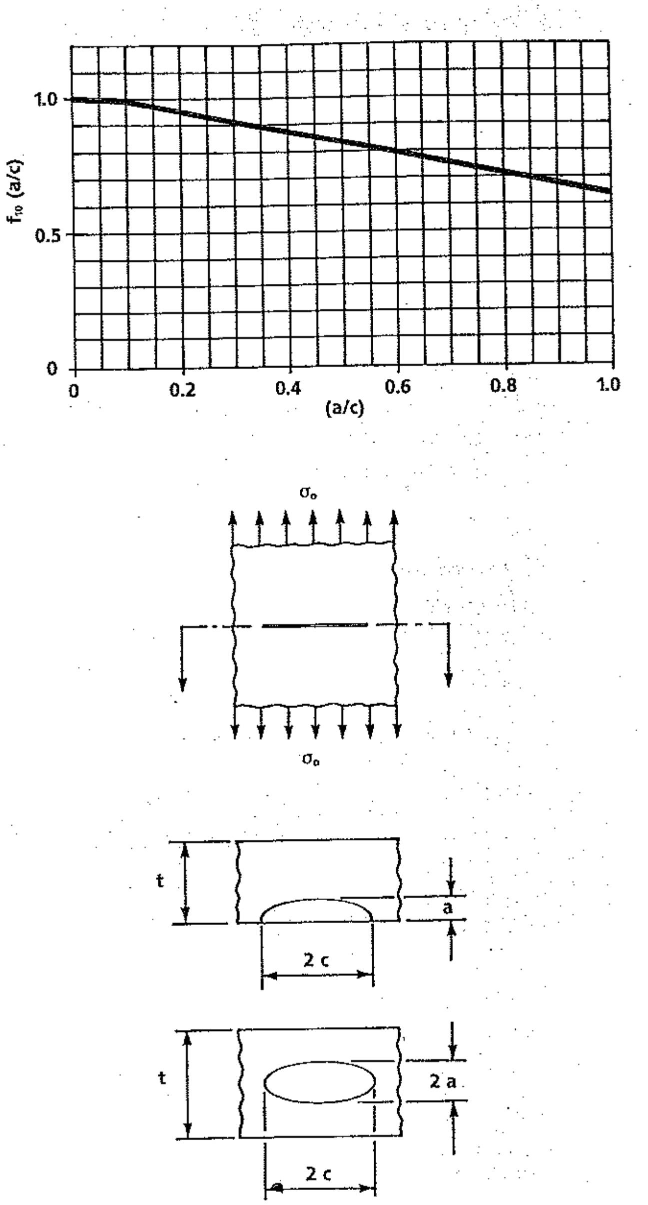

Fig. 4.7.7 *Geometry factor f_{10} (Ref. 4:34)*

Fig. 4.7.8 gives values of M_k in tension and bending for butt welds and non-loadcarrying fillet welds (Ref. 4:29). If the weld geometry is known in detail (root radius, toe angle, leg lengths and the thickness of adjoining parts), more exact expressions can be used (Ref. 4:43, 44, 48, 49).

Initial crack depth

A fracture mechanics analysis is not usually performed for the flaws which normally occur in materials or welded joints, unless these are unexpectedly large.

Various investigations show (Ref. 4:44) that defects of the order 0.3 – 0.4 mm may very well occur at the toes of normal untreated (not ground or TIG treated) butt and fillet welds. See Fig. 4.6.10.

Fig. 4.7.8 M_k for butt and fillet welds (Ref. 4:29). Note that when a/t is relatively large, say a/t > 0.2, the approximation f = 1.12 M_k is no longer valid

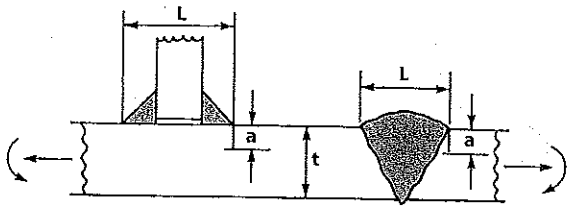

a/t				M_k in pure tension					
0.500	1.000	1.000	1.000	1.000	1.000	1.000	1.000	1.000	1.000
0.200	1.000	1.000	1.000	1.019	1.057	1.111	1.157	1.146	1.146
0.100	1.000	1.013	1.067	1.113	1.173	1.259	1.335	1.316	1.316
0.050	1.029	1.075	1.151	1.216	1.301	1.441	1.557	1.557	1.557
0.020	1.111	1.240	1.423	1.558	1.715	1.914	2.068	2.069	2.069
0.010	1.377	1.537	1.764	1.931	2.127	2.373	2.564	2.564	2.564
0.005	1.707	1.905	2.186	2.394	2.636	2.941	3.179	3.179	3.179
0.002	2.268	2.530	2.904	3.181	3.502	3.907	4.223	4.223	4.223
0.001	2.811	3.137	3.600	3.943	4.341	4.844	5.235	5.235	5.235
L/t	0.2	0.3	0.5	0.7	1.0	1.5	2.0	3.0	5.0

a/t				M_k in pure bending					
0.500	1.000	1.000	1.000	1.000	1.000	1.000	1.000	1.000	1.000
0.200	1.000	1.000	1.000	1.000	1.000	1.000	1.000	1.000	1.000
0.100	1.000	1.000	1.000	1.021	1.054	1.054	1.054	1.054	1.054
0.050	1.021	1.058	1.113	1.154	1.202	1.202	1.202	1.202	1.202
0.020	1.156	1.212	1.309	1.404	1.514	1.514	1.514	1.514	1.514
0.010	1.338	1.457	1.622	1.741	1.876	1.876	1.876	1.876	1.876
0.005	1.659	1.807	2.011	2.158	2.326	2.326	2.326	2.326	2.326
0.002	2.204	2.400	2.672	2.867	3.090	3.090	3.090	3.090	3.090
0.001	2.732	2.975	3.312	3.554	3.831	3.831	3.831	3.831	3.831
L/t	0.2	0.3	0.5	0.7	1.0	1.5	2.0	3.0	5.0

4.7.4 Fracture mechanics calculations

Will a defect grow under the action of fatigue load?

By referring to the threshold value, it is possible to calculate the maximum stress range $\Delta\sigma_{th}$ which will not propagate a known crack, or the size of crack a_{th} which will not propagate under a particular stress range.

Formula 4.7.5 gives,

$$\Delta\sigma_{th} = \Delta K_{th}/(\sqrt{\pi a}\, f) \qquad (4.7.13)$$

$$a_{th} = (\Delta K_{th}/(\Delta\sigma\, f))^2/\pi \qquad (4.7.14)$$

What size of defect is critical with respect to the risk of brittle fracture?

The critical crack size is given directly by Formulae 4.7.1 – 2:

$$a_c = (K_{Ic}/(\sigma_{max}\, f))^2/\pi \qquad (4.7.15)$$

How many load cycles are required for the defect to reach a critical size?

The Paris law can be used directly to compare the rates of growth of different cracks.

In order to calculate how many load cycles are required for growth from one crack size a_i to another a_f, the expression 4.7.6 must be integrated. The following simplifications can be made during integration:

1 Assume f = constant between increments	Use small increments initially. Vary the increment size to see which is best to yield the desired accuracy
2 Fit a polynomial to $(\sqrt{a}\, f)^{-n}$	Calculate $(\sqrt{a}\, f)^{-n}$ for a number of likely crack depths and then fit a polynomial that can be integrated easily; se Fig. 4.7.9.

Under fatigue loading, it is the *variation* in stress intensity that governs the progress of fatigue. In general, a check should also be made regarding the risk of unstable failure. The stress intensity factor must then be calculated with reference to the *maximum* nominal stress plus any residual stresses that may be present.

$$\frac{da}{dN} = C\Delta K^n = C\,[\Delta\sigma\sqrt{\pi a}\; f(a)]^n$$

$\Rightarrow$

$$\frac{da}{[\sqrt{a}\; f(a)]^n} = C(\Delta\sigma\sqrt{\pi})^n dN$$

$\Rightarrow$

$$\int_{a_i}^{a_f} \frac{da}{[\sqrt{a}\; f(a)]^n} = C(\Delta\sigma\sqrt{\pi})^n \int_{N_i=0}^{N_f} dN$$

$\Rightarrow$

$$N_f = \frac{1}{C(\Delta\sigma\sqrt{\pi})^n} \int_{a_i}^{a_f} \frac{da}{[\sqrt{a}\; f(a)]^n}$$

Calculate $\frac{1}{[\sqrt{a}\; f(a)]^n}$ for a range of 'a' values of interest, and then fit an easily integrated function to the plots. N_f is then obtained by simple integration.

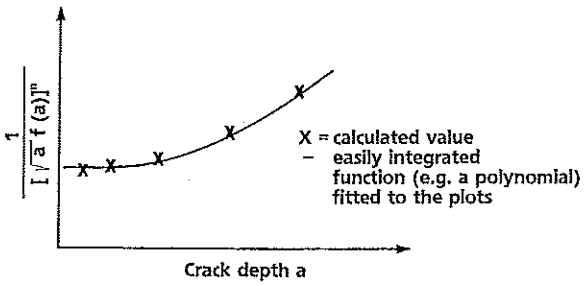

Fig. 4.7.9 *Integration of Paris law*

Defect tolerance diagrams

A defect tolerance diagram which gives approximate relationships between defect depth a and stress is given in Fig. 4.7.10. The curves for limited life have been calculated with the values n = 3 and $C = 3.9 \cdot 10^{-12}$ which are representative mean values for the products of SSAB Strip Products. The diagram is valid for a/t < 0.2 and R = 0. The geometry factor f = 1.0, and the calculations

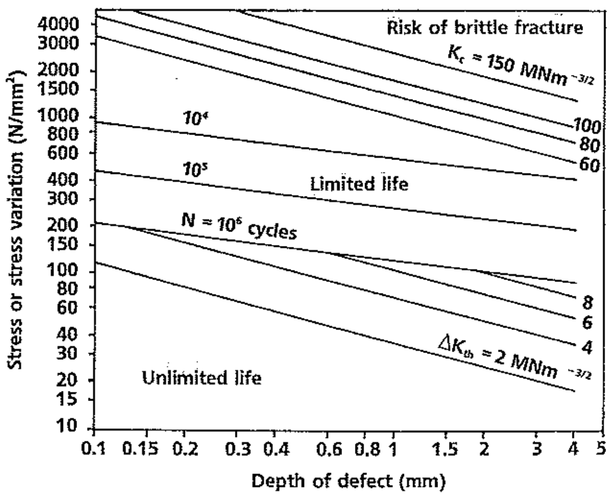

Fig. 4.7. 10 *Defect tolerance diagram (Ref. 4:47)*

hold for long internal cracks (c >> 2a), i.e. in accordance with Formula 4.7.11 b. If the geometry factor $f \neq 1$, the diagram can be entered at $f\Delta\sigma$ instead of $\Delta\sigma$. For surface cracks Formula 4.7.11 a applies, and the diagram can be entered at $1.12 f \Delta\sigma$ instead of $\Delta\sigma$ when the critical depth of defect is calculated.

The permissible depth of defect should be made 2 – 3 times smaller than the critical crack depth.

Example 4.7.1 — Permissible size of defect

A surface defect similar to a crack of approx 1 mm depth has been found in a 12 mm sheet. The length of the defect is 10 mm and it is perpendicular to the greatest stress. The sheet will be subject to a fatigue load which gives $\Delta\sigma = 60$ N/mm² and a static maximum stress $\sigma_{max} = 590$ N/mm². Can the defect be accepted if an unlimited life is required? $K_c = 60$ MNm$^{-3/2}$, $\Delta K_{th} = 6$ MNm$^{-3/2}$.

Solution

The surface crack gives

$K_I = 1.12\, \Delta\sigma \sqrt{\pi a}\, f_{10}$ (4.7.1 and 4.7.11 a)

Fatigue

$\Delta\sigma\, f = 1.12 \cdot 60 \cdot 1 = 67$ N/mm²

Fig. 4.7.10 gives the critical depth of defect. Read off the value of a_{th} at the point of intersection between $\Delta\sigma\, f = 67$ N/mm² and $\Delta K_{th} = 6$ MNm$^{-3/2}$.

$a_{th} \approx 2.4$ mm

"Brittle fracture"

$\sigma\, f = 1.12\, \sigma_{max} = 1.12 \cdot 590 = 661$ N/mm²

Critical depth of defect $a_c \approx 2.5$ mm.

Fatigue governs, and the critical size of defect is $a_{th} \approx 2.4$ mm, i.e. 2.4 times as large as the actual size. The defect of 1 mm can therefore be accepted.